5-2014

Design Optimization of a Composite Wing Box for High-Altitude Long-Endurance Aircraft

Philip T. Arévalo
Embry-Riddle Aeronautical University - Daytona Beach

DESIGN OPTIMIZATION OF A COMPOSITE WING BOX FOR HIGH-ALTITUDE LONG-ENDURANCE AIRCRAFT

By

Philip T. Arévalo

A Thesis Submitted to the College of Engineering Department of Mechanical Engineering in Partial Fulfillment of the Requirements for the Degree of
Master of Science in Mechanical Engineering

Embry-Riddle Aeronautical University
Daytona Beach, Florida
May 2014

DESIGN OPTIMIZATION OF A COMPOSITE WING BOX FOR HIGH-ALTITUDE LONG-ENDURANCE AIRCRAFT WING BOX

By

Philip T. Arévalo

This thesis was prepared under the direction of the candidate's Thesis Committee Chair, Dr. William A. Engblom, Professor, Daytona Beach Campus, and Thesis Committee Members Dr. Jean-Michel Dhainaut, Professor, Daytona Beach Campus, and Dr. Sathya Gangadharan, Professor, Daytona Beach Campus, and has been approved by the Thesis Committee. It was submitted to the Department of Mechanical Engineering in partial fulfillment of the requirements for the degree of Master of Science in Mechanical Engineering

Thesis Review Committee:

William A. Engblom, Ph. D.
Committee Chair

Jean-Michel Dhainaut, Ph. D.
Committee Member

Sathya Gangadharan, Ph. D.
Committee Member

Darris L. White, Ph.D.
Graduate Program Chair,
Mechanical Engineering

Charles F. Reinholtz, Ph.D.
Department Chair,
Mechanical Engineering

Maj Mirmirani, Ph.D.
Dean, College of Engineering

Robert Oxley, Ph.D.
Associate Vice President of Academics

5-28-14
Date

Acknowledgements

The author acknowledges the University as a whole for providing a substantial environment for his personal, educational, and professional development since the Fall of 2006.

The author also acknowledges the numerous contributions of the thesis committee in the development of this thesis, and is grateful.

The encouragement and support of the friends and family of the author toward the completion of this thesis are recognized and greatly appreciated.

The author gives special thanks to Vladislav Shulmann, Fyderyk Pomirski and Carolynne Lewis-Arévalo for their assistance in preparation for the defense and report.

Abstract

Researcher: Philip T. Arévalo

Title: Design Optimization of a Composite Wing Box for High-Altitude Long-Endurance Aircraft

Institution: Embry-Riddle Aeronautical University

Degree: Master of Science in Mechanical Engineering

Year: 2014

A design optimization process is developed to define the wing box structure for High-Altitude Long-Endurance Aircraft (HALE). The goal of this study is to determine the best tradeoff between mass and rigidity of a HALE aircraft wing structure. A preliminary composite laminate structural design procedure is described which uses a NASTRAN-based Finite Element Analysis (FEA), and the Hierarchical Evolutionary Engineering Design System (HEEDS) MDO software to define a locus of acceptable, optimized wing box design definitions.

Table of Contents

List of Tables

List of Figures

1. Introduction

Current High-Altitude Long-Endurance (HALE) aircraft have limited station keeping ability, normally due to the use of consumable fuels. In an attempt to solve this problem, W.A. Engblom developed the Dual-Aircraft Atmospheric Platform (DAAP) for HALE station-keeping which is explained in [1]. DAAP is a new flight concept that consists of two glider-like unmanned aerial vehicles (UAVs) connected via a thin tether (see Figure 4) and uses persistent stratospheric wind shear to remain aloft indefinitely [1]. To determine the feasibility of DAAP, Eric M. McKee designed an aircraft to fulfill the requirements of DAAP. The object of this thesis is to develop an aircraft wing design and optimization methodology that would apply to HALE aircraft as well as provide analysis based data for a DAAP reassessment.

2. Literature Review – HALE

High Altitude Long Endurance (HALE) aircraft are in increased use today. For example, NASA has two programs which use Global Hawk aircraft to study weather systems [3] and [4]. NASA has performed research into the development of HALE aircraft that are not dependent on consumable fuels [5] with the HELIOS program. [5] also describes the catastrophic failure of the fragile wing structure of the HELIOS HP03 when encountering gusts after a modification to conquer long endurance goals. [6] describes the Solar Impulse, a solar powered aircraft that performs night flights with an alternate wing design that incorporates a wing box which has not been destroyed. However, due to depletion of batteries during the night, it is incapable of station-keeping.

Figure 1 – Global Hawk UAV implemented by NASA [3]

Figure 2 – HELIOS aircraft developed for non consumable fuel HALE flights [5]

Figure 3 – Solar Impulse [6]

3. Literature Review - Structural Optimization

[7] describes the relation of detail of analysis models to the computational power of the era and the necessity of efficiency in modeling for design. [8] introduces an optimization methodology in which the plies of a composite laminate have fixed orientation, but can vary in thickness, a useful method for preliminary sizing projects. [9] and [10] describe a highly detailed design optimizations which includes the stacking, orientation and thickness of each ply, as well as the optimization software HEEDS to perform multidisciplinary design optimizations.

4. Reference Aircraft

4.1. DAAP

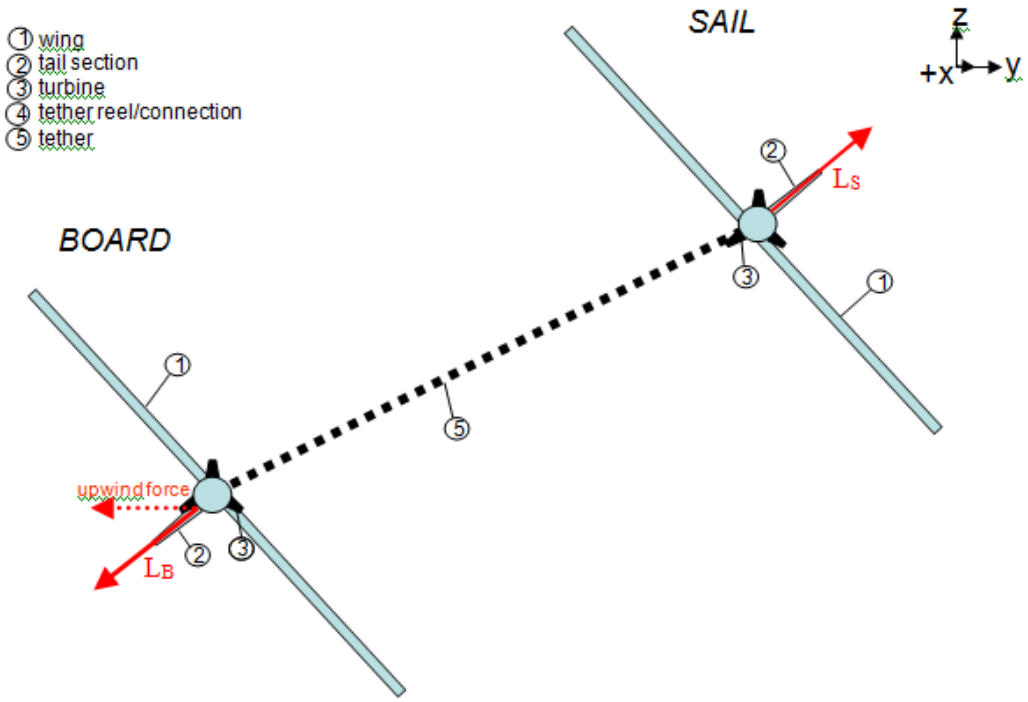

Figure 4 - Artist rendering of DAAP [1]

The DAAP model, developed by W.A. Engblom, consists of two aircraft that are tethered together which use stratospheric wind shear to generate lift and thrust with the intention of station-keeping. According to [1], DAAP operates at approximately 60,000 ft where the winds are steady but have sufficient variance to allow the two aircraft to orient themselves in such a way to stay aloft. Wind conditions were investigated over two locations twice daily for a year, and this information was entered into the DAAP model. The number of cases in which the DAAP model could find an orientation solution for the entire year's worth of data is called operability. The operability results are below in Figure 5.

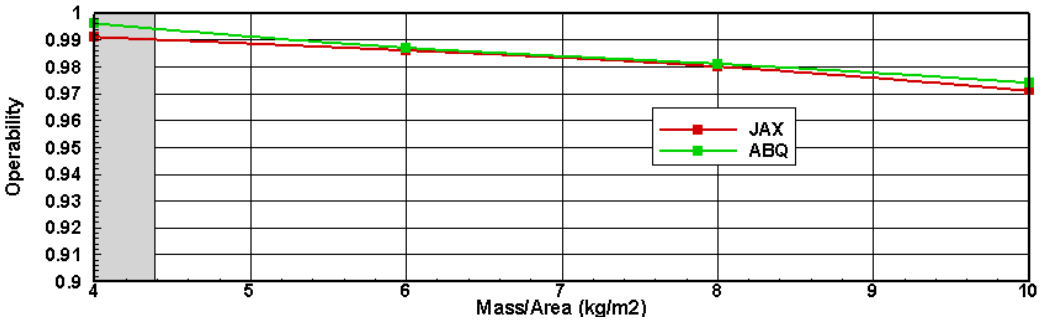

Figure 5 – Initial DAAP operability assessment [1]

Figure 5 shows the results of the DAAP operability assessment as a function of Mass/Area of the aircraft. Per Figure 5, the lighter the aircraft, the better the operability. At 4 kg/m^2, the DAAP model achieves 99% operability. These values are theoretical since the airframe has not yet been designed. To obtain a higher fidelity assessment of the DAAP model, a preliminary aircraft design was conceived.

4.2. DAAP Aircraft Design

Eric M. McKee completed the design of the aircraft for the DAAP model, which is pictured below in Figure 6

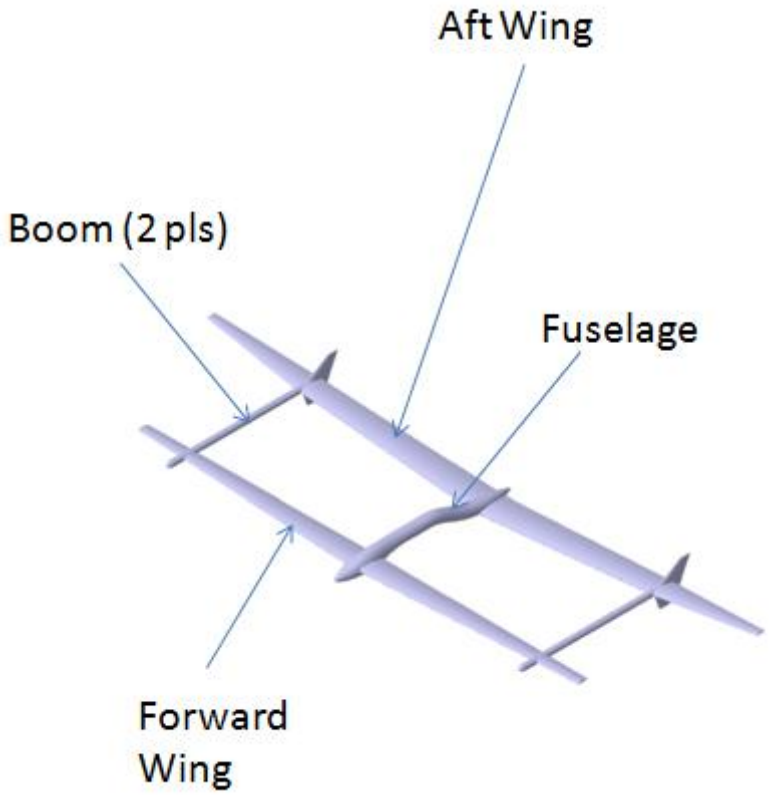

Figure 6 – Isometric view of DAAP aircraft ([2])

From Figure 6, we see that the aircraft is a tangent bi-plane with a maximum wing span of 100ft (≈ 30.5m) and a reference area of 423ft^2 (≈ 39.3m^2) on the aft wing. The aft wing is the larger of the two, and generates most lift; therefore it will be the subject of this thesis. Since the forward wing will not be analyzed in this thesis, the boom to which it attaches will not be analyzed either.

The aft wing is composed of two separate sections, the inboard section and the outboard section, the geometric properties of which are detailed in the following table.

Table 1 – Geometric properties of aft wing sections

Wing Section	Inboard	Outboard
Half Span	9.7 m	5.4 m
Root Chord (Cr)	2138	1283
Tip Chord (Ct)	1283	472
Leading Edge Sweep	0	4.7
Dihedral	5.5	5.5

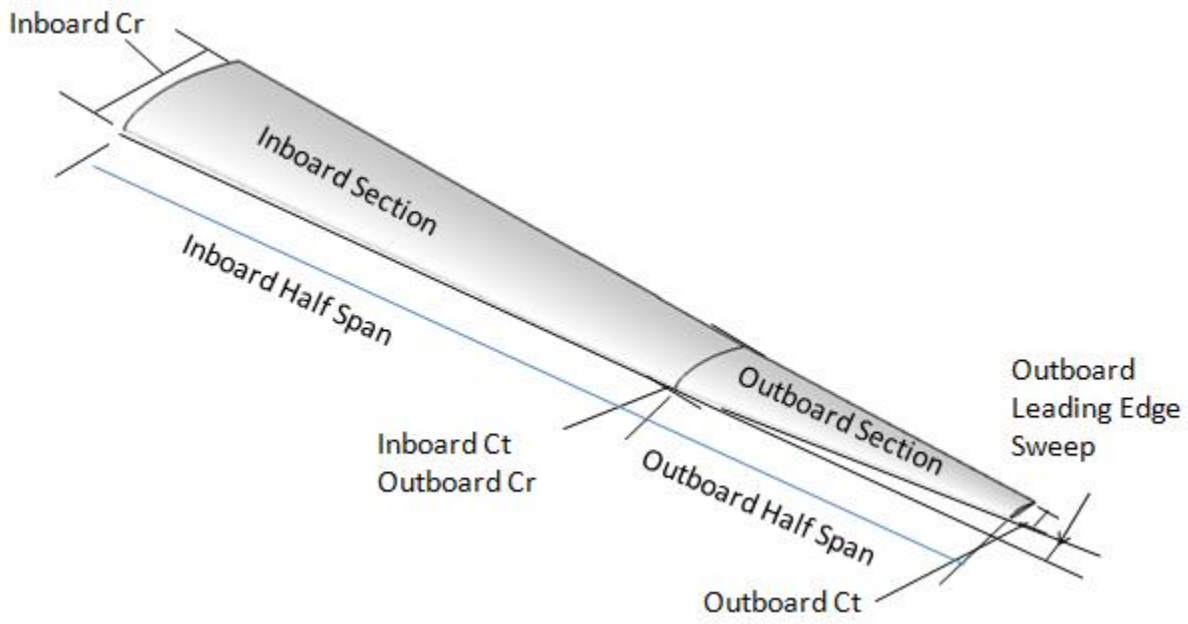

Figure 7 – Left hand side aft wing sections

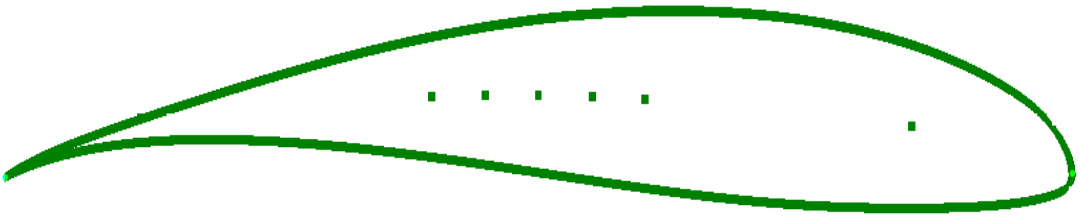

Figure 8 – Profile of the Wortmann FX 63-137

The airfoil used on both sections of the wing was the Wortmann FX 63 137. This airfoil was selected by McKee for its gentle stall characteristics and wide drag bucket.

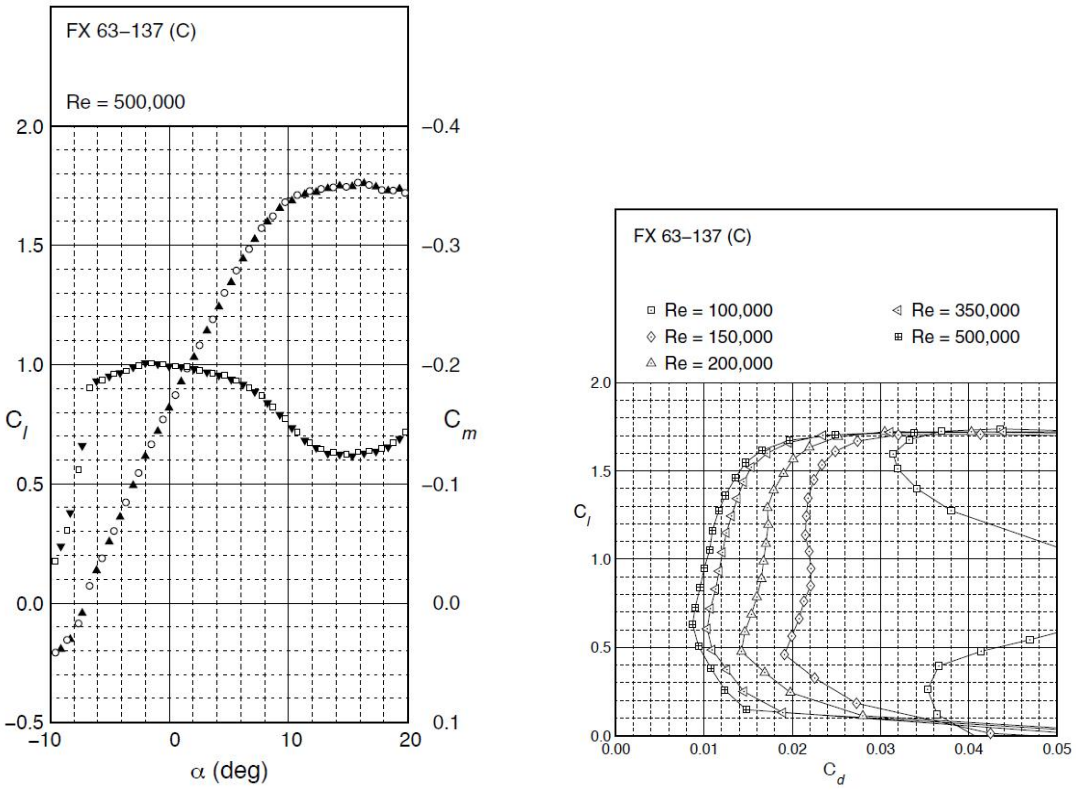

Figure 9 – Lift and drag polars for the Wortmann FX 63-137 [2]

From Figure 9, the gentle stall indicates that instead of a sudden drop in lift after the aircraft stalls, it has maintains a relatively high lift coefficient. The wide drag buckets indicates that as the lift increase the wing maintains relatively low drag. Regardless of the fact that there are airfoils with higher lift coefficients, both aforementioned qualities make the Wortmann ideal for operating at the wide range of angles of attack seen by the DAAP model.

5. Mission

This thesis defines an efficient methodology of designing a HALE aircraft wing box structure with a balance between aerodynamic performance and the mass of the wing, which can be applied to any mission requirements. Additionally, this thesis provides data for a reassessment of the DAAP model.

6. Goals

1. Create a starting point for optimization by creating a structural baseline design of the wing box
2. Generate a lift loss vs. mass plot for multiple allowable wing tip deflections

7. Methodology

This thesis uses a two-phase process to achieve its goals. The first phase is to develop the design of the baseline wing box, and the second phase is to generate the lift loss vs. mass plot.

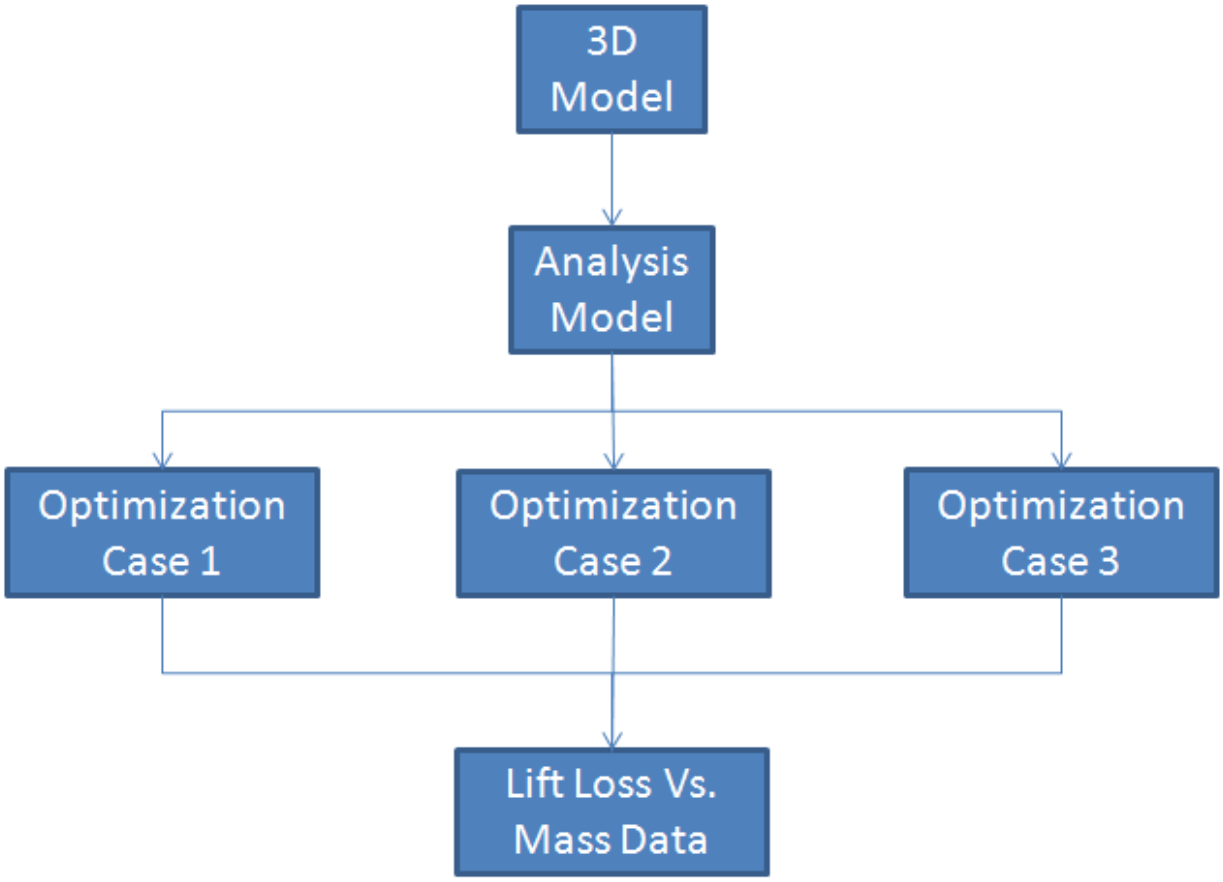

Figure 10 – Methodology flow chart

Phase one develops the design of the baseline wing box by generating a model of the wing in the Computer Aided Three-dimensional Interactive Application (CATIA) based on the reference aircraft in §4. Then, a finite element model (FEM) of the wing box is created in FEMAP/NX NASTRAN to analyze the structure. Two studies are run to determine the best configuration of spars and ribs. Then, the layup for the baseline design is determined.

Phase two finds the relationship between lift-loss and mass by optimizing the wing box structure at three allowable deflections cases. Then, for each deflection case, the lift loss is calculated. Finally, the values of minimum mass and the lift loss at each tip deflection are compared to reveal the relationship between lift-loss and mass.

7.1. Structural Components of a Wing Box

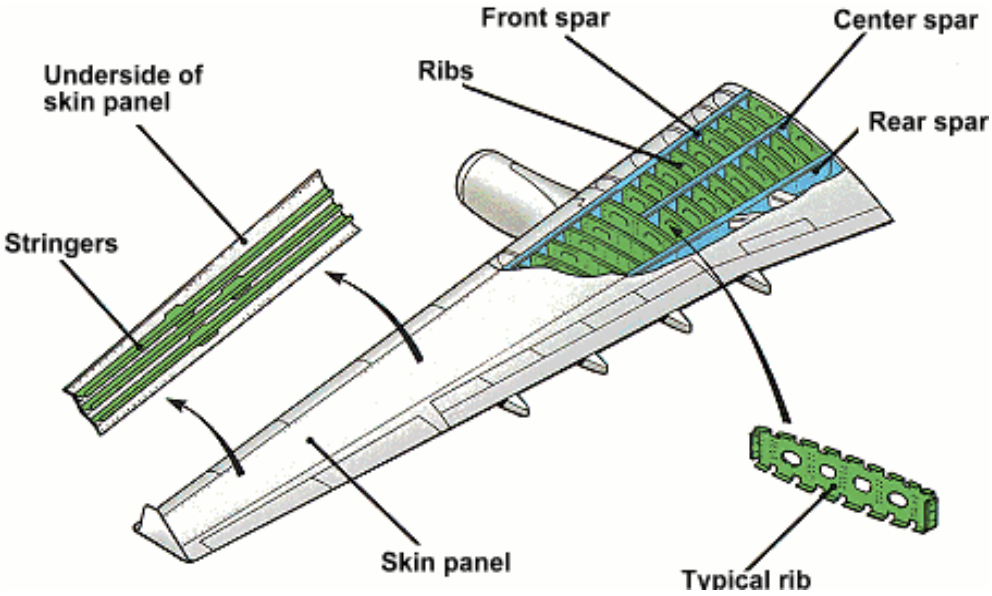

Figure 11 – Structural components of a wing box with labels [11]

A wing box is made of 3 structural members: wing skin, spars, and ribs. The wing skin can aid in the reaction of bending moments, but it primarily carries shear loading. Skin panels are located on the top and bottom of the wings. Spars are members that run along the span of the wing and react carry bending and shear loads from lift. The ribs run across the spars and they give form to the wing covers as well as prevent buckling of the wing covers.

7.2. Materials

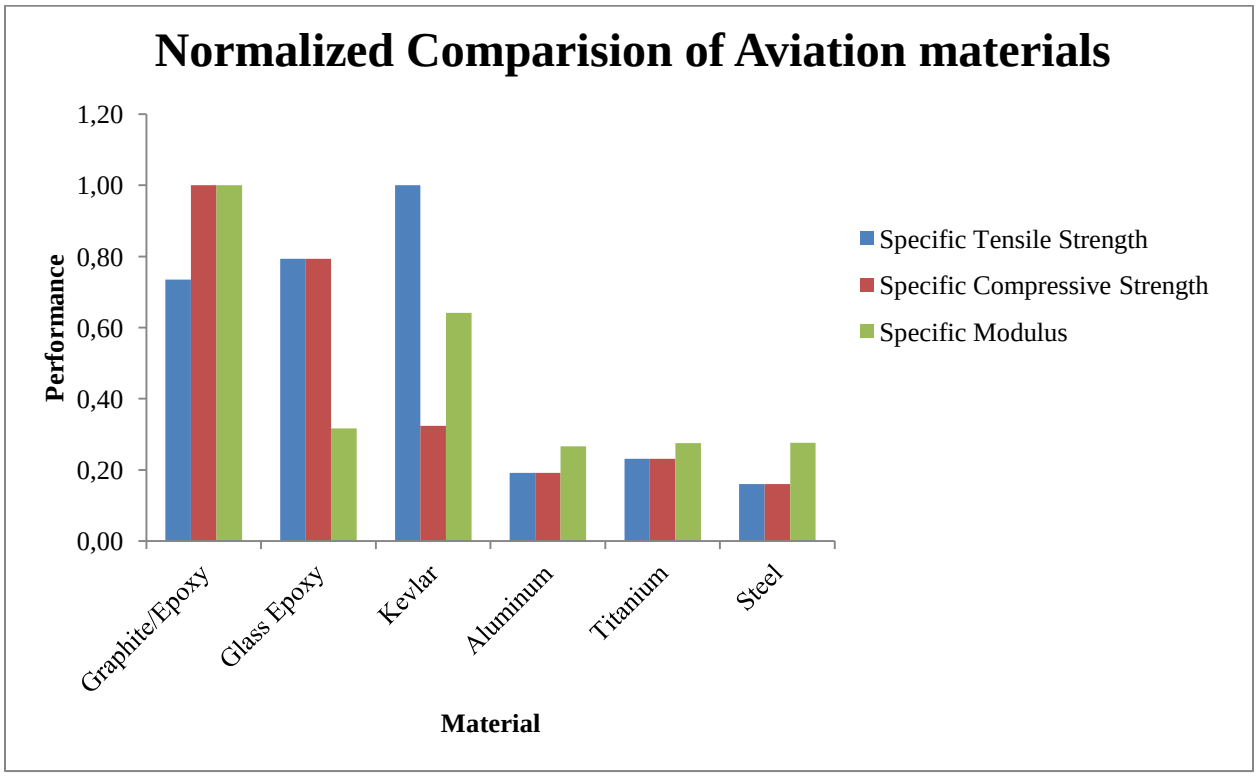

Figure 12 – Comparison of aerospace materials

The aim for this project is to achieve a very light weight and rigid structure. The desired material can be selected by referring to the specific strength and the specific modulus. These are factors which compare the strength and stiffness to the weight of the materials. In cases where high strength and very low weight are required, a high specific strength is suitable. In cases where a high stiffness and low weight are concerned, a high specific modulus is suitable. This aircraft needs both, therefore the best material to use is CFRP. Shown in the graph, this material offers the best overall values for specific strength and specific modulus.

There are two ways to use composites, in monolithic structure, or in sandwich composite structures. Monolithic indicates that the layup is purely the composite material. Since the strength to weight ratio is very high, this requires less material. The thin profile of components made of CFRP can lead to structural instability, or buckling. In order to prevent buckling the moment of inertia can be increased by the addition of a core material, which leads to sandwich composites.

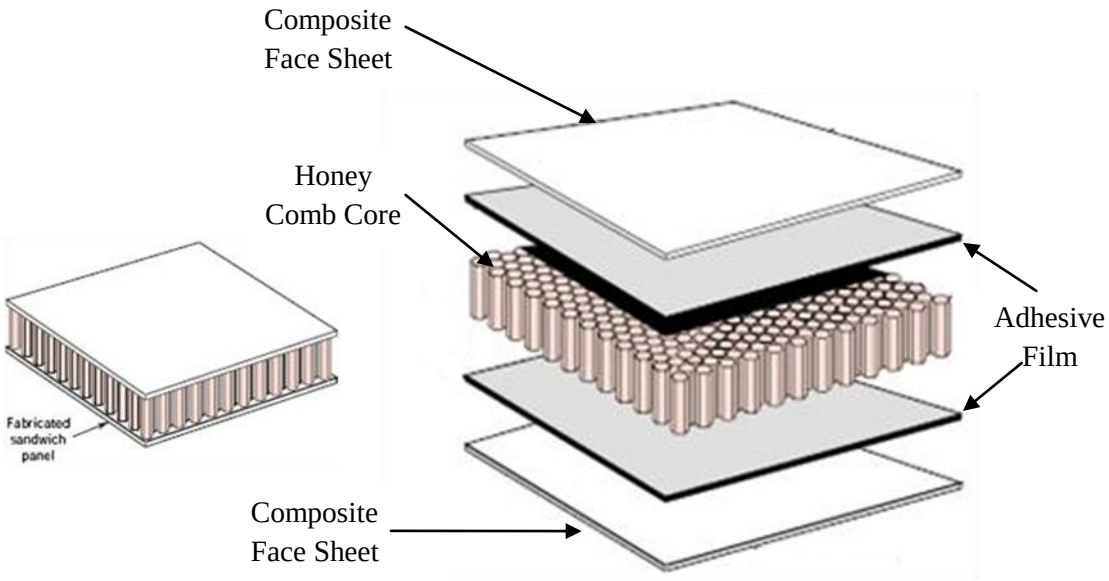

Figure 13 – Diagram of sandwich composite

A sandwich composite material consists of face sheets made of a highly stiff and very strong composite material, a lightweight core material, and adhesive film to hold the two together. The role of the face sheets is to take in-plane loads. Since the face sheet has such high specific modulus and specific mass, it may only require a few plies which make it susceptible to buckling. The role of the lightweight core material is to make the layup more stable by increasing its thickness, which inherently increases the moment of inertia. The second role of the core material is to carry out-of-plane shear loads. Generally, in high stress conditions, a material that is formable and that has high shear strength is used.

7.3. Layup Definition of Composite Honeycomb Panels on Wing Box

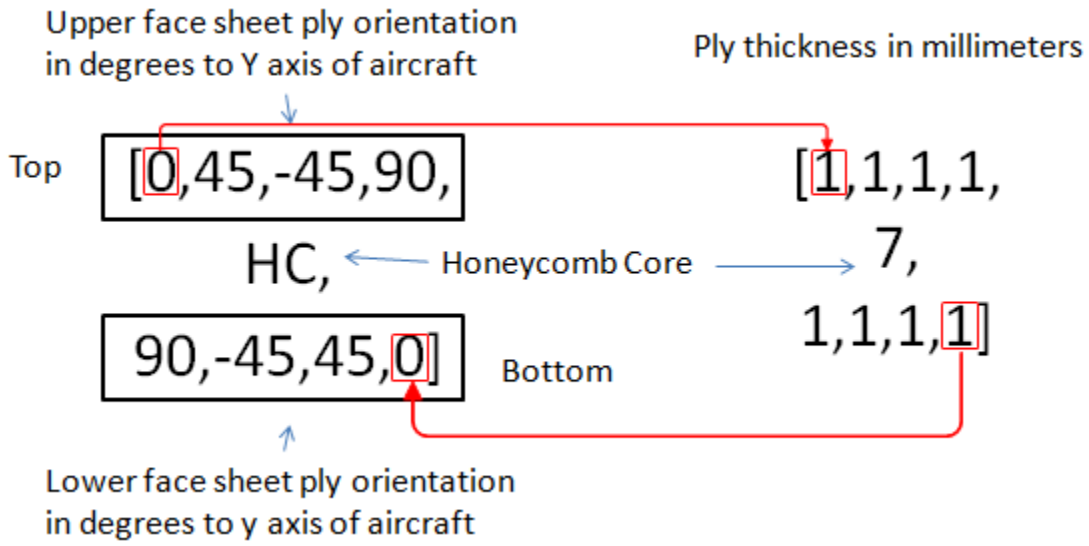

The layup definition of the composite honeycomb plies is defined above. The y axis is used as the reference from which the orientations of the plies are set. An orientation of zero degrees indicates a ply with its fibers running along the span of the wing, and likewise for the rest of the plies. The upper section indicates the orientations of the plies which make up the upper face sheet of the layup. At the center is the honeycomb core, and on the bottom is the lower face sheet. On the right are the thicknesses associated with each ply. The design and optimization use a symmetric layup with a honeycomb core for all sections of the wing box.

7.4. Requirements for a Feasible Design

For this thesis, a feasible design is one that when subjected to loading will demonstrate static strength and structural stability. Static Strength will be determined when comparing the stresses in the structure to the allowable limits of the materials. Structural stability is determined by how susceptible the structure is to buckling. This is determined by using a buckling eigenvalue, which is a factor that when multiplied by the current loading system, yields the loading at which the structure will buckle.

Additionally, the design with regard to the DAAP assessment requires the output of the mass of the structure and the wing tip deflection. This information will also be investigated.

7.5. Finite Element Analysis

Finite Element Analysis (FEA) is a numerical computation method that is used to analyze complex structures. FEA takes large bodies and breaks them into smaller finite elements. This is done because these finite elements are governed by mechanics equations that are simpler to solve than the one needed to analyze the entire structure. A computer can run many more simplified equations quickly, which makes these finite elements models ideal for analysis. These finite elements are given the material and geometric properties that would exist on the actual structure. Loads and constraints are applied to the model to simulate the operating environment. Then, the finite element solver calculates the strains, stresses, deflections, and other desired output of the structure under the load case. The FEA software used in this model is NX NASTRAN with a FEMAP pre/postprocessor. FEMAP is the user interface in which the user creates, runs, and post-processes analyses that are calculated in NX NASATRAN.

7.5.1. Mesh Creation

Studying mesh size for a model helps to find an accurate and reliable model. It is important to run a study to determine the size of the mesh. The number of elements in a FEM is related to the precision attained. It is important to use just enough elements to have a precise model. With too many elements, the computation time is greatly increased and efficiency is lost. The number of elements needed for an accurate estimation of a model's results is determined using a mesh independent study. During the study, one of two parameters changes, either the number of elements or the size of the elements. With each change to the mesh, the values are studied for convergence. When the values converge within a given range, say 1%, the study is complete.

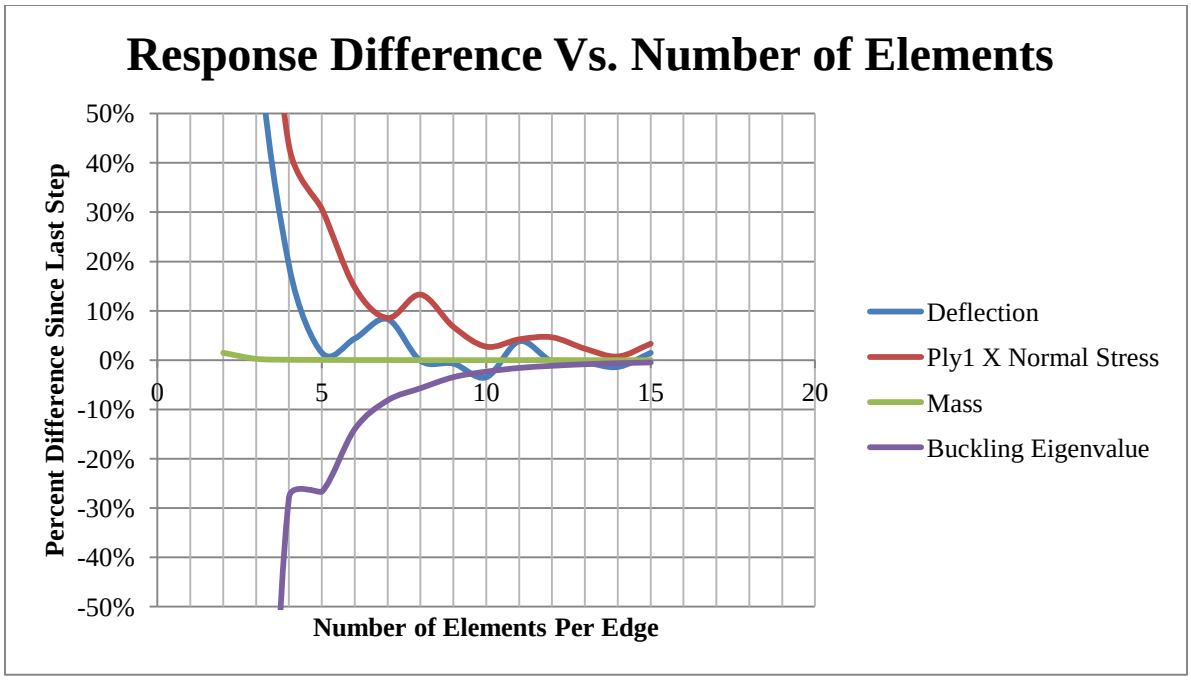

Figure 14 - Response difference vs. number of elements

Figure 14 shows a chart graphing the results from a mesh independent study of a sample section of the AFT wing of the DAAP airframe. The percent difference is calculated by the current step result values subtracted from the previous step result. The difference between the values is then divided by the average of the two values as shown in the equation below.

$$\%diff = \frac{(Previous\ Value - Current\ Value)}{\left(\frac{Previous\ Value + Current\ Value}{2}\right)} \times 100$$

From Figure 14, the convergence of the response values reaches ±1% when the number of elements per edge is 14.

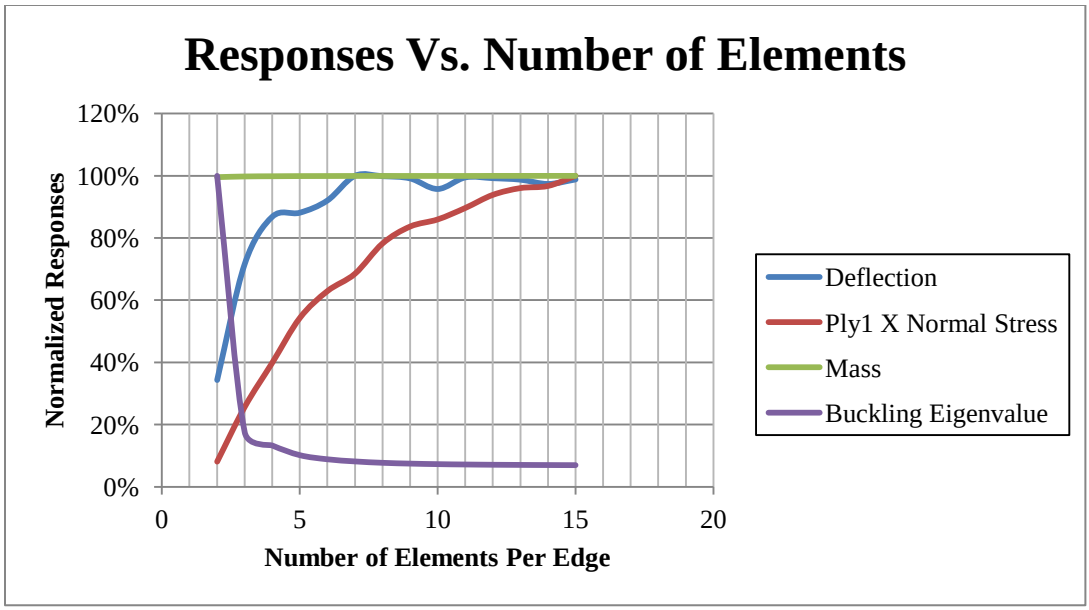

Figure 15 - Normalized response values vs. number of elements per edge

Figure 15 graphs the normalized responses from the FEA against the number of elements per edge. There is local oscillation among the responses as the number of edge elements changes; this is normal. The global trend of the responses demonstrates that they converge. The convergence dictates that the ideal number of elements along the edge of the wing is 14 for the analysis. This number of elements is translated into a mesh size, and is applied to the whole model (~65mm).

7.6. Wing Loading

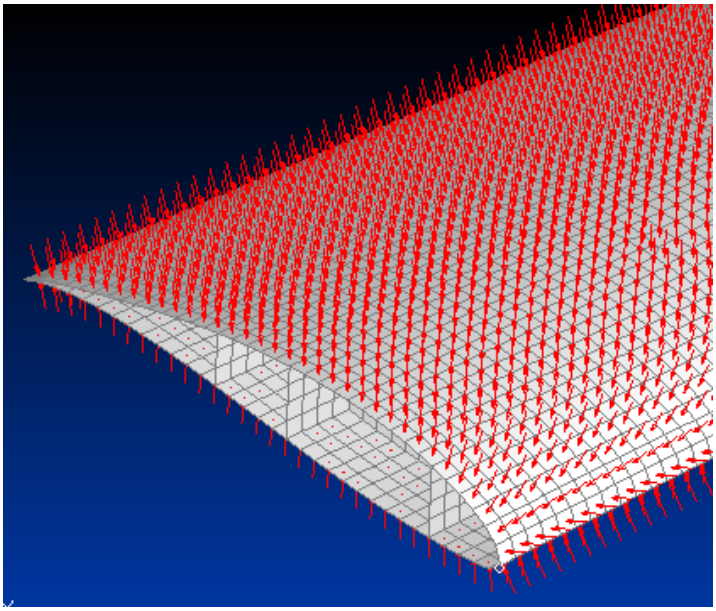

Figure 16 – Representation of pressure loads applied on FEA mesh

A wing is loaded based on the aerodynamic pressure during flight. In the case of this wing, the pressure loads across the wing were calculated using a CFD analysis run by W.A. Engblom. Then, a MATLAB code originally developed by ERAU students, Michael Borghi and Fumbi Kolawole, was adapted and used to read in CFD pressure data on a Cartesian grid, and to them to FEA pressure loads on the FE mesh. This M-code also prints out each pressure load card in NASTRAN bulk data format. The loads were calculated at the maximum angle of attach for the aircraft of 13.5 degrees from [2] at the cruise velocity.

7.7. FEA Buckling

The results for an FEA buckling analysis are interpreted as an eigenvalue which is usually represented by the Greek letter λ, and is used in the following equation

$$P_{Cr} = \lambda P$$

Where P_{Cr} is the critical buckling load and P is the load on the structure. In this case the buckling eigenvalue λ is the ratio between the critical buckling load and the current load. The value of the eigenvaule states whether the structure is buckled under the current loading as such:

$$if \quad \lambda \geq 1 \quad Buckling\ Occurs$$

$$if \quad \lambda < 1 \quad No\ Buckling$$

7.8. Failure Criterion

To determine the static strength of the structure, the materials are compared to the material limits. One way to do this is called the max stress or strain method. In this method, the stress or strain in one direction is compared to that allowable. This is only acceptable if the structure is loaded in one direction. When the structure is loaded in multiple directions, the interaction of stresses changes the failure limit for the structure. One method that considers this is the Tsai-Wu Criterion which is given by the following equation:

$$f_1\sigma_1 + f_2\sigma_2 + f_{11}\sigma_1^2 + f_{22}\sigma_2^2 + f_{66}\tau_6^2 + 2f_{12}\sigma_1\sigma_2 = 1$$

Where:

$$f_1 = \frac{1}{F_{1t}} - \frac{1}{F_{1c}} \qquad f_{11} = \frac{1}{F_{1t}F_{1c}}$$

$$f_2 = \frac{1}{F_{2t}} - \frac{1}{F_{2c}} \qquad f_{22} = \frac{1}{F_{2t}F_{2c}}$$

$$f_{66} = \frac{1}{F_{66}} \qquad f_{12} \cong -\frac{1}{2}\sqrt{f_{11}f_{22}}$$

And
F_{1t}: Tensile Strength of Fiber Direction
$F_{1c:}$ Compressive Strength of Fiber Direction
F_{2t}: Tensile Strength of Matrix Direction
$F_{2c:}$ Compressive Strength of Matrix Direction
F_6: Shear Strength
σ_1: Stress Direction of Fibers
σ_2: Stress Direction of Matrix
τ_6: Shear Stress

The failure of a material based on the Tsai-Wu Criterion occurs when the sum of the components is equal to 1. The advantage of the Tsai-Wu Criterion is that it accounts for the failure based on interaction of stresses and that it intrinsically accounts for compression or tension limit values. For these reasons, the Tsai-Wu criterion is selected for this thesis.

8. Wing Box Structural Design

The wing box structural design comprises three steps, one for the spar configurations, one for the rib configurations and one for the layup used for each wing box component.

8.1. Spar Study

8.1.1. Aft Spar 60% FWD Spar 15%

The fwd spar location can be determined by where the highest pressure loads are concentrated, and the shear center, which is defined as the location at which a load can be applied which results in no twist of the structure. Due to limited data of the pressure loads throughout the range of angles of attack, the spar location study based on this method is postponed. Using [12] as a guide, the forward spar is located at 15% for the entire study. The aft spar is affected by the sizing of the control surfaces. In the case of DAAP these have not yet been determined. Therefore, using [12], the aft spar can vary between 60% and 50%.

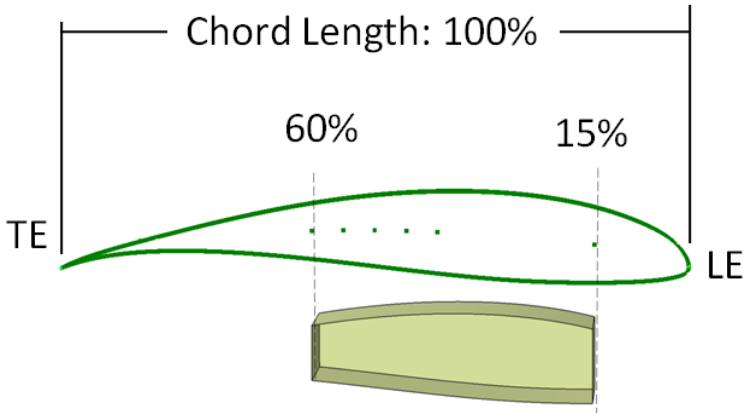

Figure 17 – View of first spar configuration AS 60% FS 15%

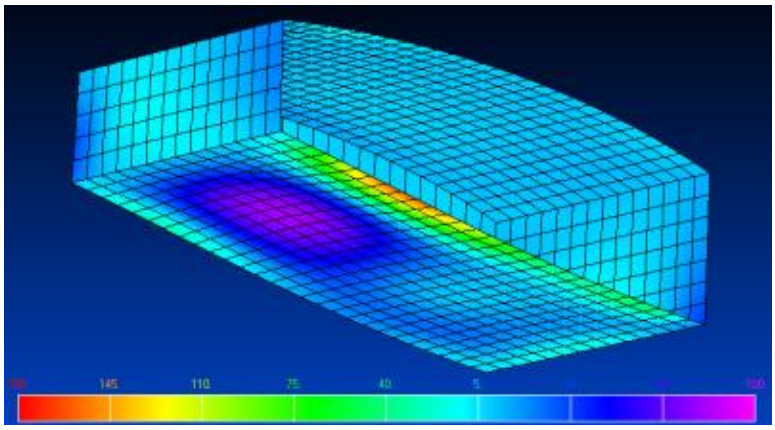

Figure 18 – FEA results on first configuration

Table 2 – Results first spar study

Deflection (mm)	15.03
Stress (MPa)	164.2
Mass (kg)	4.50
Buckling Eigen Value	0.33

The first configuration indicates high stress in the wing cover. To resolve this issue, the aft spar was moved forward to see if the stress was reduced.

8.1.2. Aft Spar 55% FWD Spar 15%

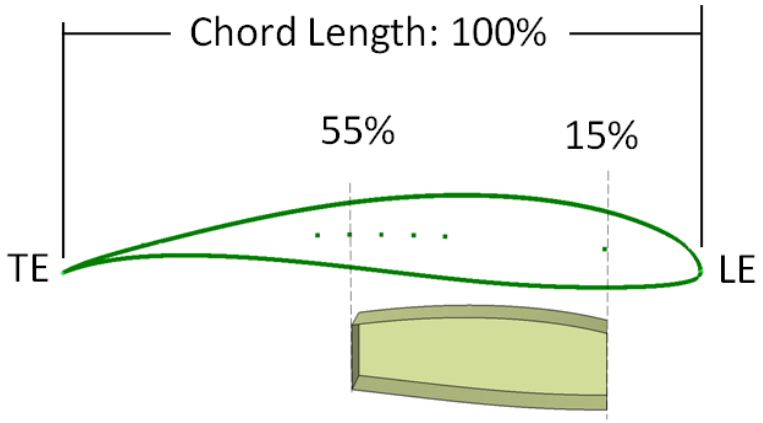

Figure 19 – View of second spar configuration AS 55% FS 15%

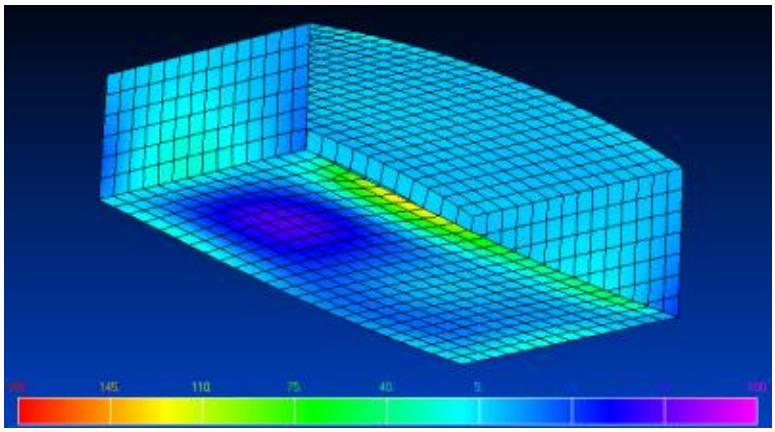

Figure 20 – FEA results on second configuration

Table 3 – Results of second spar study

Deflection (mm)	11.42
Stress (MPa)	135.8
Mass (kg)	4.14
Buckling Eigen Value	0.34

It can be seen that the stress does go down when moving the spar forward. Further investigation is carried out in the next step.

8.1.3. Aft Spar 50% FWD Spar 15%

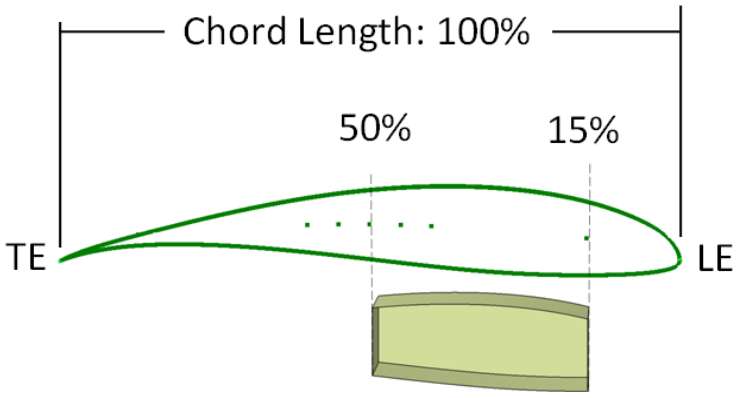

Figure 21 – View of third spar configuration AS 50% FS 15%

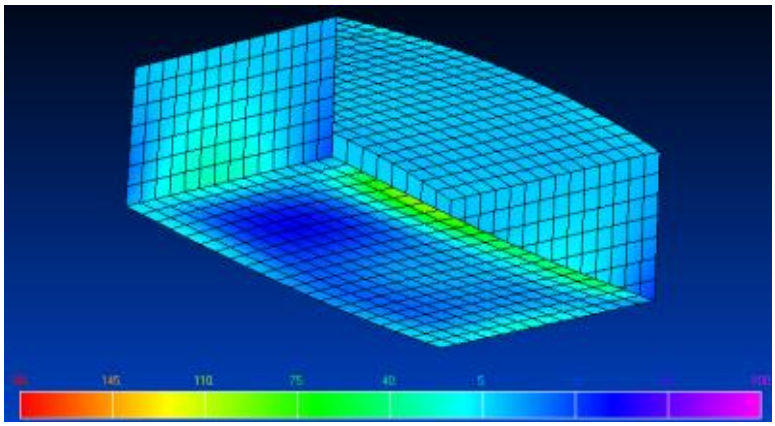

Figure 22 – FEA results on third configuration

Table 4 – Results of third spar study

Deflection (mm)	8.04
Stress (MPa)	106.4
Mass (kg)	3.76
Buckling Eigen Value	0.38

In this spar study, the decrease in stress is very interesting. Advancing the aft spar may lead to lower stress in the lower wing cover. However, 45% is not covered by the guidelines. Therefore the 4th configuration adds an extra spar to maintain the guideline.

8.1.4. Aft Spar 60% Mid 45% FWD Spar 15%

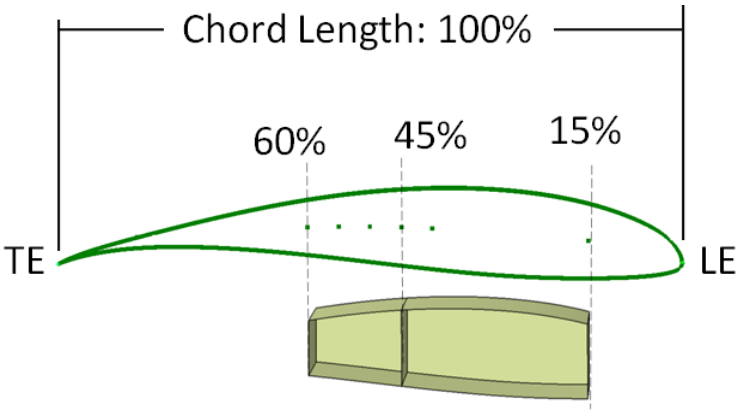

Figure 23 – View of fourth spar configuration AS 60% MS 45% FS 15%

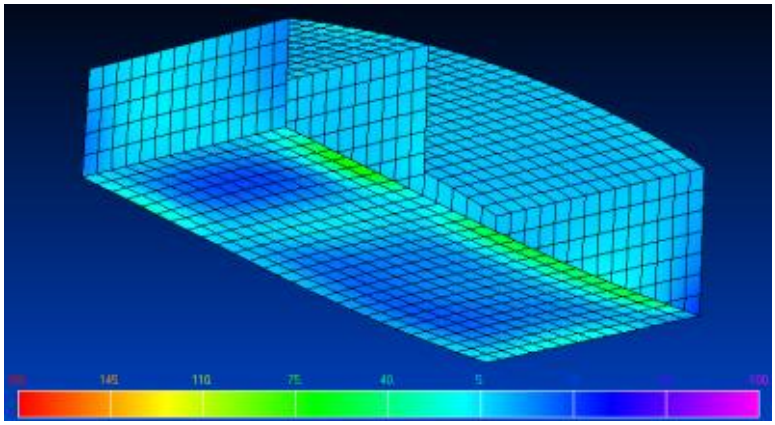

Figure 24 – FEA results on fourth configuration

Table 5 – Results of fourth spar study

Deflection (mm)	6.72
Stress (MPa)	83.8
Mass (kg)	4.91
Buckling Eigen Value	0.46

The addition of the third spar was a success in reducing stress in the material. This design is expanded upon with the next iteration. It appears that there is a curvature change in the lower wing cover which induces the high stress. Adding the additional mid spar at 45% acts to support this curvature

change. The study is continued to determine if the stresses go down again if the mid spar is moved forward again.

8.1.5. AFT Spar 60% Mid 40% FWD Spar 15%

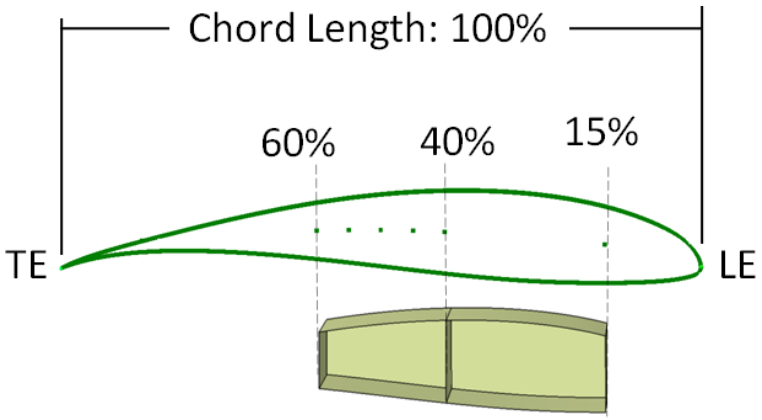

Figure 25 – View of fifth spar configuration AS 60% MS 40% FS 15%

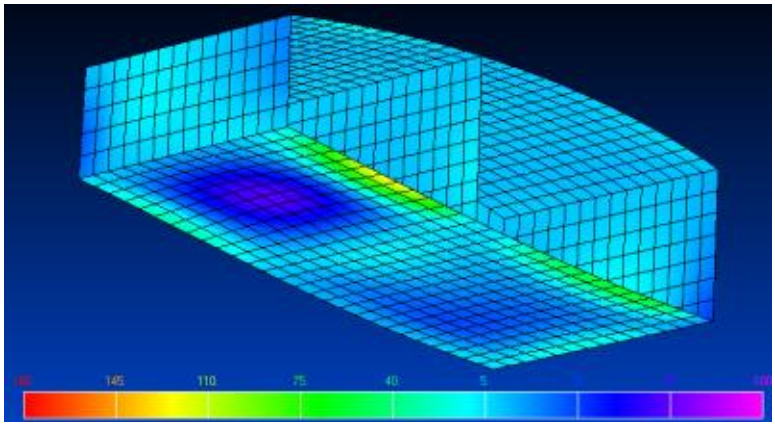

Figure 26 – FEA results on fifth configuration

Table 6 – Results of fifth spar study

Deflection (mm)	11.70
Stress (MPa)	133.3
Mass (kg)	4.93
Buckling Eigen Value	0.55

The stress increases in this configuration therefore the study is ended and the results are compared. The results are compiled together and compared to determine the best design.

8.1.6. Spar Study Summary

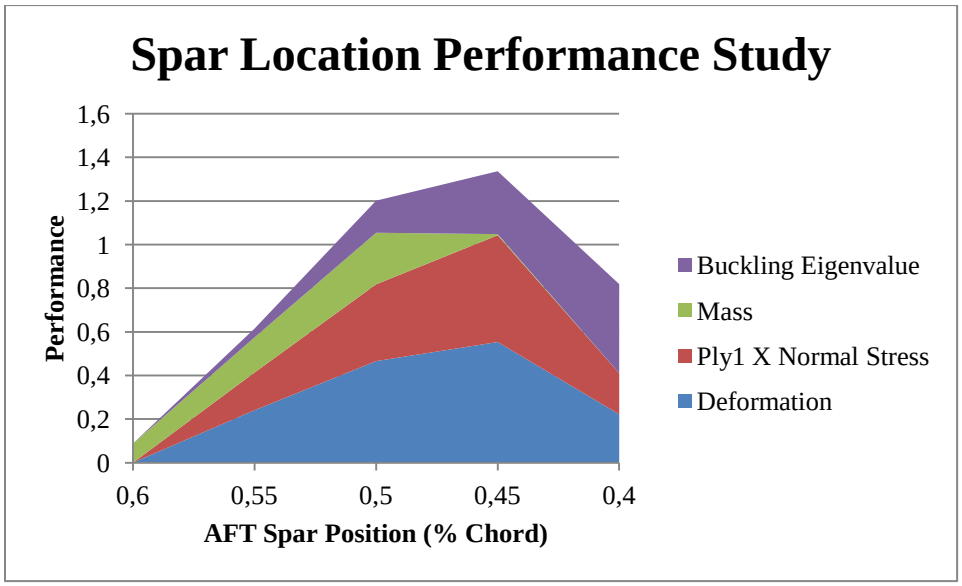

Figure 27 – Spar study results

For the spar study, the results were compared and normalized to each to other. The results when compared to each other yielded the information in Figure 27. From this graph it is clear that the tri-spar configuration with the mid spar at 45% is the best design. This is selected and used for the baseline design.

8.2. Rib Spacing Study

The rib spacing is determined by varying the spacing between the ribs and the results of the mass, buckling Eigenvalue, the deflection, and the stress are compared to determine which spar configuration has the best performance. The rib spacing distances compared are 250mm to 1250mm by increments of 250mm. The study is conducted in the same fashion as the spar study with the variable being the spacing between the ribs.

Table 7 – Rib spacing study results

Spacing	250mm	500mm	750mm	1m	1.25m
Configuration	1	2	3	4	5
Deformation (mm)	1.157	6.721	10.78	13.93	**23.62**
Stress (MPa)	36.89	83.8	97.48	151.1	**207.3**
Mass (kg)	**110.97**	95.70	90.34	87.45	85.55
Buckling Eigenvalue	3.02	0.46	0.25	0.19	**0.17**

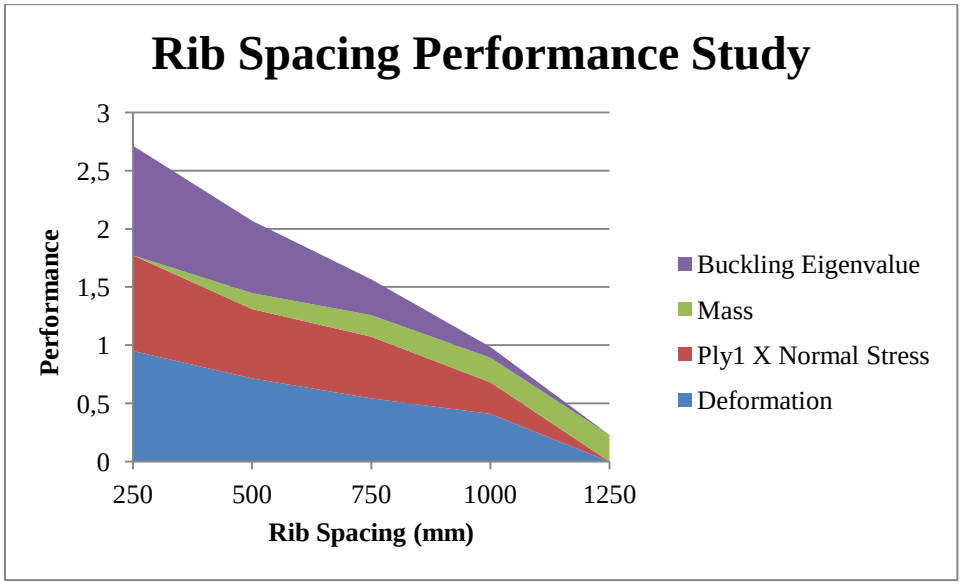

Figure 28 - Rib spacing performance study

The rib spacing with the largest normalized performance is the configuration 1 at 250mm between ribs. Rib configurations with less than 250mm spacing would result in a design that would be too heavy. Therefore, the 250mm spacing is selected, and the rest of the wing is built according to these data. Now that the configuration of the wing is setup, the baseline design can continue. It is noted that this methodology is biased toward the heaviest design. Using engineering judgment, the study was terminated at the 250mm case.

8.3. Layups

The initial baseline design was determined using a manual approach. The number of plies and orientation and thickness were assigned according to the stress levels in the structure based on visual inspection of the FEM in post-processing and assessment of the failure index. The plies of each section inboard, midboard, and outboard have a progressive step down in the number of plies used while maintaining a symmetric layup, the final definition of which are described in the following sections. Below is a breakdown of the three wing section partitions.

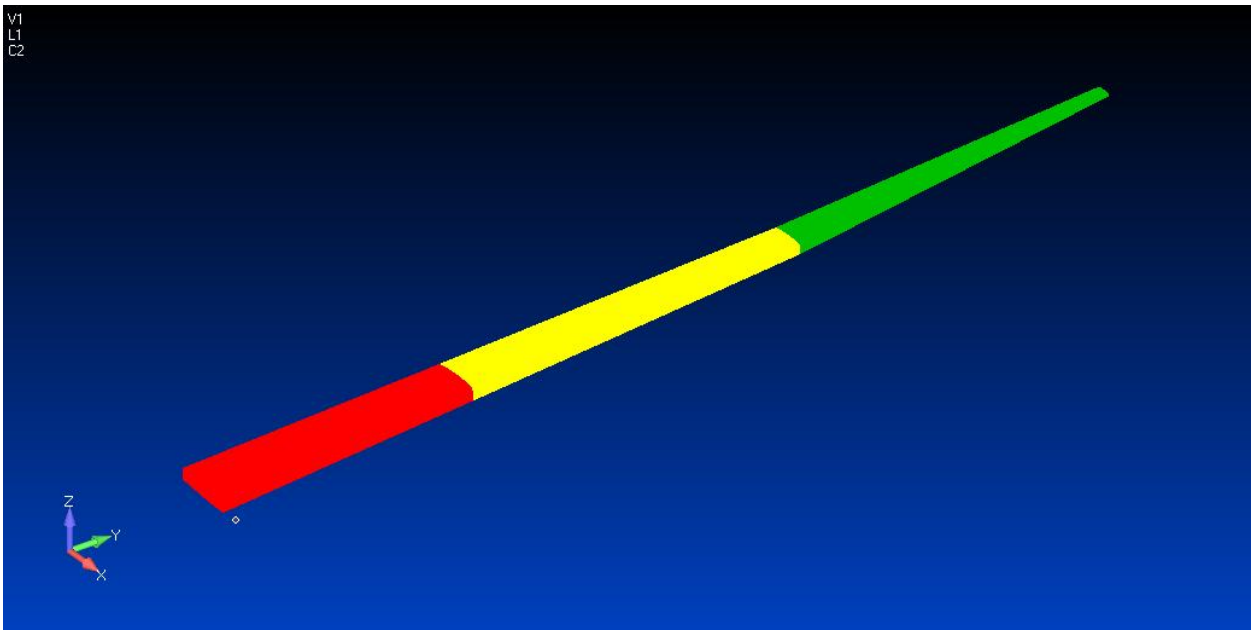

Figure 29 - Wing Sections

In Figure 29, the wing box is divided into 3 sections. Each section is given its own layup, which is sized based on the local stresses in its section. The small dot represents the origin or the root of the wing. Therefore the inboard section (1) is highlighted in red. The midboard section (2) is represented in yellow and the outboard section (3) is highlighted in green. The inboard section runs between the root of the wing and the 16th rib. The midboard section runs between the 16th rib and the 22nd rib, and the outboard section runs between the 22nd rib and the tip of the wing. Then, each of these sections is divided into the components of the wing, Wing Cover (C), Spar (S), and Rib (R), thus creating 9 individual layups for the entire wing.

Table 8 – Laminate Summary

C1_T0	Thickness of the plies in the C1 Layup oriented at 0 degrees
C1_T45	Thickness of the plies in the C1 Layup oriented at 45 degrees
C1_T90	Thickness of the plies in the C1 Layup oriented at 90 degrees
C1_T_Core	Thickness of the honeycomb core in the C1 Layup
C2_T0	Thickness of the plies in the C2 Layup oriented at 0 degrees
C2_T45	Thickness of the plies in the C2 Layup oriented at 45 degrees
C2_T_Core	Thickness of the honeycomb core in the C2 Layup
C3_T0	Thickness of the plies in the C3 Layup oriented at 0 degrees
C3_T90	Thickness of the plies in the C3 Layup oriented at 90 degrees
C3_T_Core	Thickness of the honeycomb core in the C3 Layup
S1_T0	Thickness of the plies in the S1 Layup oriented at 0 degrees
S1_T45	Thickness of the plies in the S1 Layup oriented at 45 degrees
S1_T90	Thickness of the plies in the S1 Layup oriented at 90 degrees
S1_T_Core	Thickness of the honeycomb core in the S1 Layup
S2_T0	Thickness of the plies in the S2 Layup oriented at 0 degrees
S2_T45	Thickness of the plies in the S2 Layup oriented at 45 degrees
S2_T_Core	Thickness of the honeycomb core in the S2 Layup
S3_T45	Thickness of the plies in the S3 Layup oriented at 45 degrees
S3_T_Core	Thickness of the honeycomb core in the S3 Layup
R1_T_45	Thickness of the plies in the R1 Layup oriented at 45 degrees
R1_T_Core	Thickness of the honeycomb core in the R1 Layup
R2_T_45	Thickness of the plies in the R2 Layup oriented at 45 degrees
R2_T_Core	Thickness of the honeycomb core in the R2 Layup
R3_T_45	Thickness of the plies in the R3 Layup oriented at 45 degrees
R3_T_Core	Thickness of the honeycomb core in the R3 Layup

8.4. Summary of Baseline Design

8.4.1. Configuration

After the spar and rib studies, the final model was designed using the collected data. The aft wing has three spars: the front spar is located at 15% chord, the mid spar is located at 45% chord, and the aft chord is located at 60% chord length. The rib spacing was determined to be 250mm. The final number of ribs is 59.

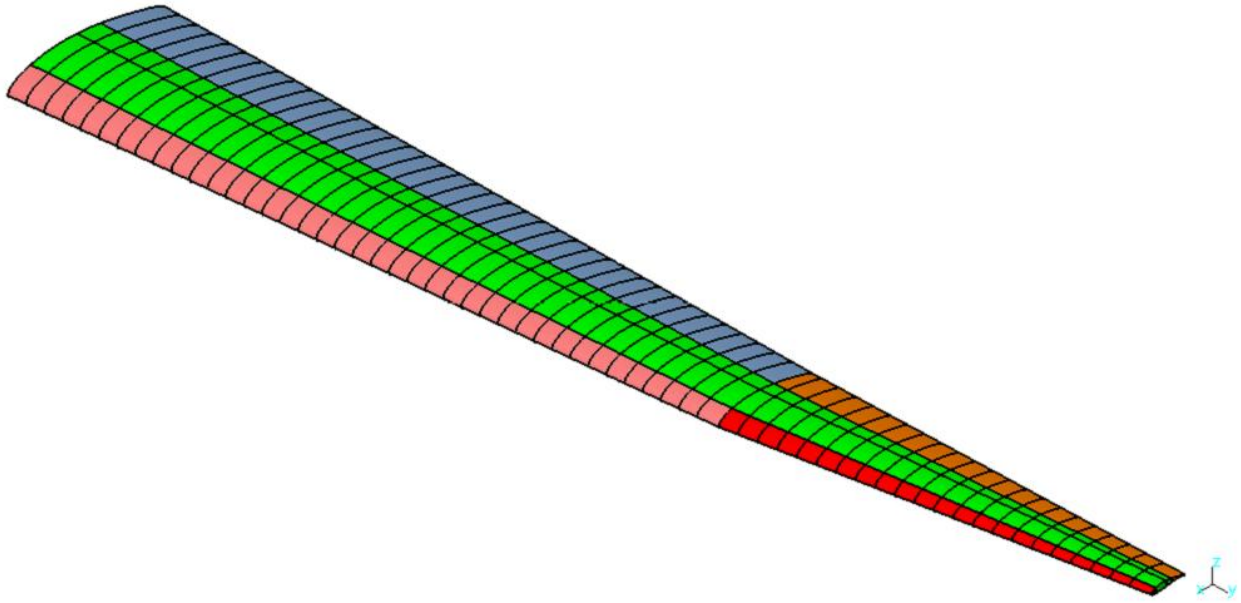

Figure 30 - Aft wing 3D model final version

8.4.2. Results

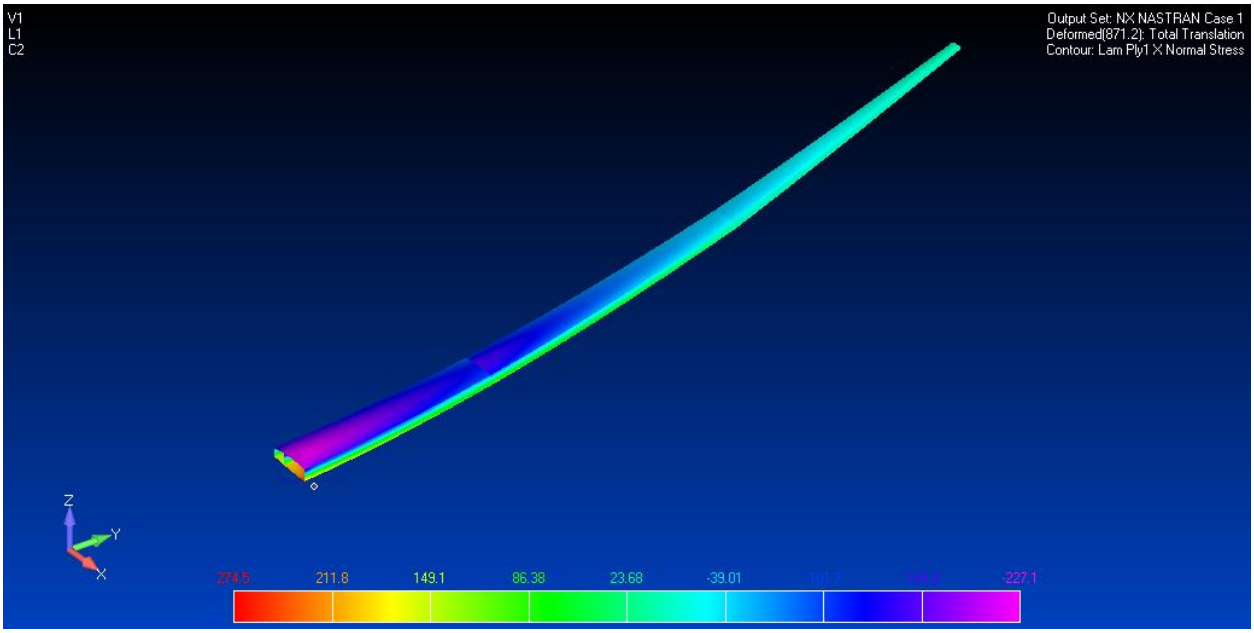

Figure 31 - FEA results for baseline design

Table 9 – Baseline design response values

Failure Index	0.623	< 1 Feasible
Buckling Eigenvalue	1.35	> 1 Feasible
Tip Deflection (mm)	871	-
Mass (kg)	251	-
Mass per unit area (kg/m3)	11.78	-

The design is feasible since the failure index is less than 1 and the buckling Eigenvalue is greater than 1. It is additionally important to notice that the starting mass per unit area is higher than what DAAP can produce and must therefore be reduced. This is done using optimization.

9. Optimization

9.1.1. Objective Function

Minimize:	Mass
Subject to:	$f_1\sigma_1 + f_2\sigma_2 + f_{11}\sigma_1^2 + f_{22}\sigma_2^2 + f_{66}\tau_6^2 + 2f_{12}\sigma_1\sigma_2 < 1$
	$\lambda > 1.1$
	Case 1 Deflection < 500mm
	Case 2 Deflection < 1000mm
	Case 3 Deflection < 2000mm
By changing:	Ply thicknesses (Table 10)

9.1.2. Optimization Details

The objective is to minimize the mass of the design while it is subject to a failure index less than 1, an Eigenvalue greater than 1.1 and by modifying the thickness of the plies of the 9 layup sections.

The failure index constraint is taken to be 1 according to the Tsai-Wu Criterion. The buckling Eigenvalue constraint is set to be 1.1, which leaves a 10% margin above the critical buckling load. The deflection constraint is different for each case. The wing is optimized at 3 deflection limits to study the effects of having wings of varying flexibility. The deflections are 0.5m, 1m, and 2m. The constraints on the ply thicknesses were determined for an upper and a lower value. First, the design was manipulated for feasibility, which is shown as the baseline design parameters from the baseline design study. Then, the upper limits to the thickness were set to be just a little larger than the baseline. The lower limits were set to be the thinnest available thickness for a CFRP ply 0.25mm.

The optimization is stopped when the improvement from one iteration to another changes by only 1 percent.

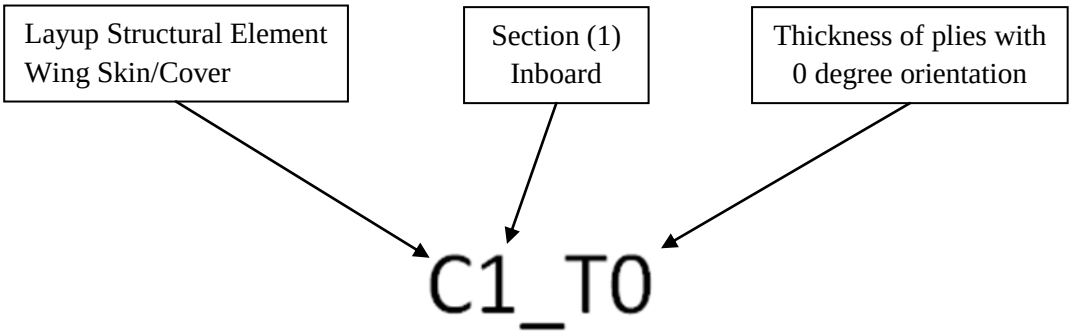

Figure 32 – Nomenclature for design variables

Table 10 – Variable Definition

Variable	Minimum (mm)	Baseline (mm)	Maximum (mm)
C1_T0	0.25	1	1.25
C1_T45	0.25	1	1.25
C1_T90	0.25	1	1.25
C1_T_Core	0.25	7	8
C2_T0	0.25	1	1.25
C2_T45	0.25	0.25	0.45
C2_T_Core	0.25	5	6
C3_T0	0.25	1	1.25
C3_T90	0.25	0.25	0.5
C3_T_Core	0.25	5	6
S1_T0	0.25	0.25	0.5
S1_T45	0.25	1	1.25
S1_T90	0.25	0.25	0.5
S1_T_Core	0.25	5	6
S2_T0	0.25	0.25	0.5
S2_T45	0.25	1	1.25
S2_T_Core	0.25	5	6
S3_T45	0.25	1	1.25
S3_T_Core	0.25	5	6
R1_T_45	0.25	0.25	0.5
R1_T_Core	0.25	5	6
R2_T_45	0.25	0.25	0.5
R2_T_Core	0.25	5	6
R3_T_45	0.25	0.25	0.5
R3_T_Core	0.25	5	6

1. C1 – Wing Cover of the Inboard Section
2. C2 – Wing Cover of the Midboard Section
3. C3 – Wing Cover of the Outboard Section
4. S1 –Spar of the Inboard Section
5. S2 –Spar of the Midboard Section
6. S3 – Spar of the Outboard Section
7. R1 –Rib of the Inboard Section
8. R2 –Rib of the Midboard Section
9. R3 –Rib of the Outboard Section

9.2. HEEDS

Hierarchical Evolutionary Engineering Design System (HEEDS) is an optimization software developed by Red Cedar Technology, and it uses the Simultaneous Hybrid Exploration that is Robust, Progressive and Adaptive (SHERPA), which is a proprietary optimization search method that they developed. Working with many software programs, HEEDS can create completely automated optimizations by sharing data between separate analyses and launching programs in succession. This is ideal for Multi-Objective Optimizations which require several different analyses.

9.2.1. Search Method

The advantage of using HEEDS and the SHERPA method is the fast and thorough exploration of the design space relative to other search methods. An experiment demonstrating the effectiveness of HEEDS SHERPA compared to other optimization algorithms was undertaken by Red Cedar Technology, and results are displayed in Figure 33 below.

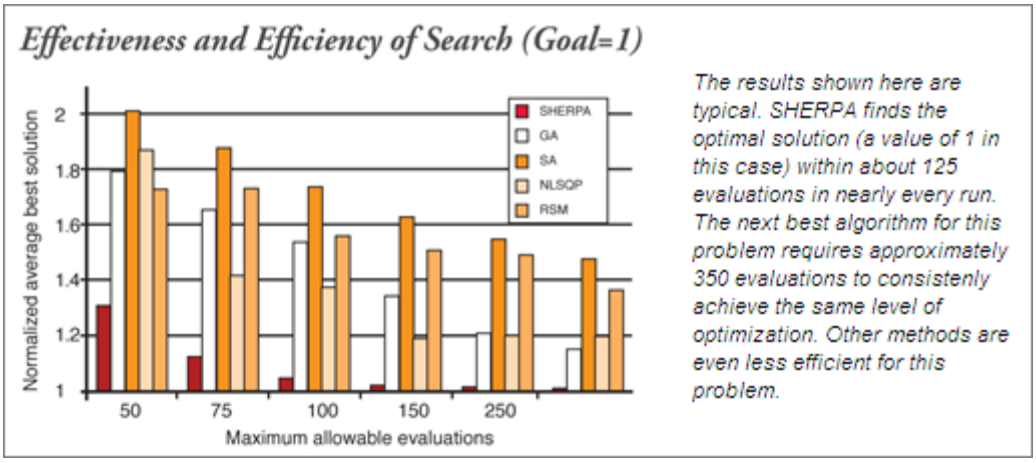

Figure 33 - Effectiveness and efficiency results from SHERPA method compared to other methods of optimization

Figure 33 shows a side by side comparison of the optimization effectiveness and efficiency of the SHERPA Method compared to other optimization search methods such as the generic algorithm and simulated annealing. The vertical axis represents the normalized average of the best possible solution. The optimal solution is 1. The horizontal axis represents the number of evaluations. Reading the chart left to right, this shows how many evaluations performed by each search algorithm to arrive at the optimal solution. Clearly, the SHERPA method out performs all other search methods.

9.2.2. Automation

The second advantage of using HEEDS is automation. HEEDS executes the optimization by running a series of scripts that activate and run CAE models to manipulate the design variables, extract the responses, and search for the optimal design. In the case of this thesis, HEEDS is used to open a NASTRAN file and a MATLAB file in series. The FEA is handled in the NASTRAN process, where the mass, stresses, stability and deflection are determined. The next step in the process is the failure criterion, which is run in a MATLAB code. This code imports the NASTRAN calculated stress data, calculates the failure criterion for each ply, and then exports the maximum failure criterion. HEEDS runs these two steps in series and collates the results.

9.3. Results

Table 11 – Optimization information

Case	500 mm	1m	2m
Number of iterations	265	126	173

Table 12 – Optimized design response values

Allowable deflection case	Baseline	500 mm	1m	2m
Failure index	0.623	0.287	0.727	0.941
Bucklin eigenvalue	1.35	1.533	1.110	1.102
Tip deflection attained (mm)	871	500	1000	**1206**
Mass (kg)	251	267	195.5	178.5
Mass per unit area (kg/m^2)	12.80	13.59	9.95	9.08

It is clear that the mass decreases as the allowable tip deflections increase. It is important to note, the case for limiting the deflection at 2m did not attain the 2m deflection due to being limited by buckling at 1205.93mm.

10. Lift Loss Estimation

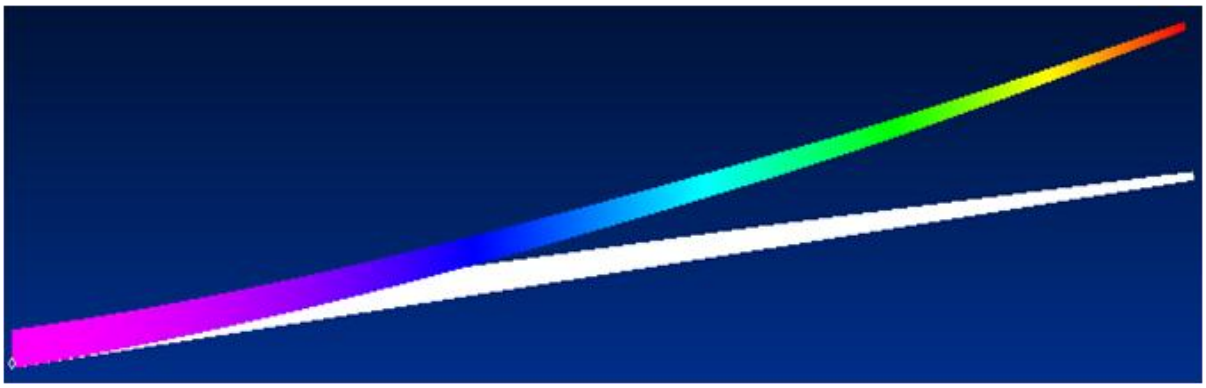

Figure 34 - Deformed and undeformed wing

Figure 34 shows a deformed wing compared to a non-deformed wing. The white section indicates the wing that is undeformed, i.e. before loading. The effect of the deflection is a change in the angle of the cross-section of the wing, which changes the vector of the pressure force. This effect changes the magnitude of the lift component of the pressure force.

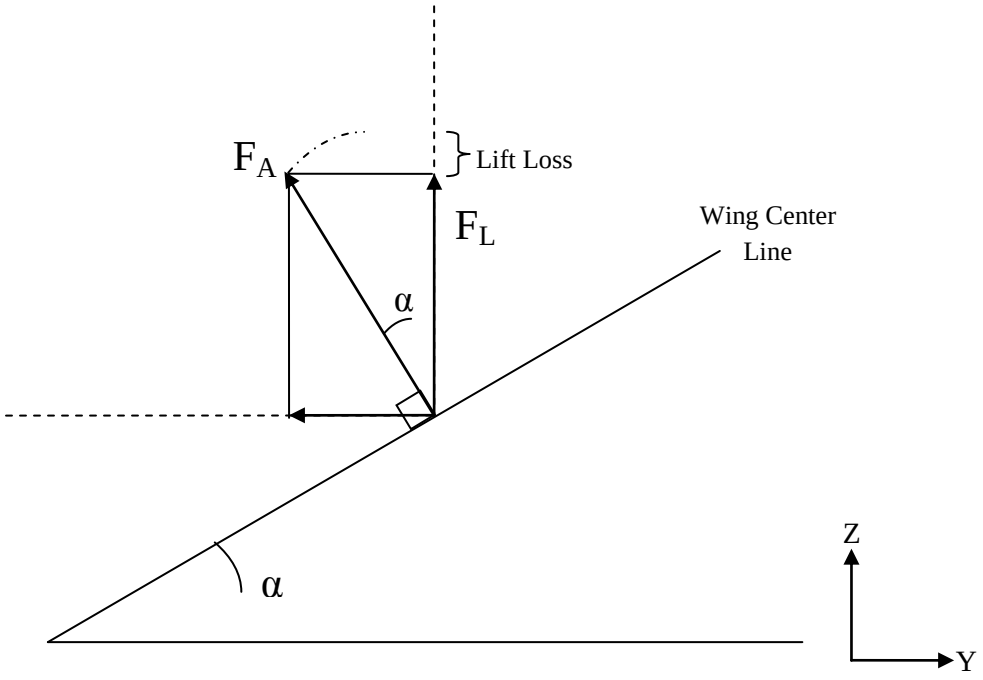

Figure 35 - Lift loss image

When considering the Y/Z plane normal to the flight velocity, the lift force is a component of the resultant aerodynamic forces on a wing as given by the following equation.

$$F_L = F_A \cos\alpha$$

Lift loss due to wing tip deflection is assumed to be the difference between the resultant aerodynamic force on the wing and the lift force actually experienced.

Therefore

$$Lift\ Loss = F_A - F_L$$

Substituting the lift equation into the lift loss equation yields:

$$Lift\ Loss = F_A - F_A \cos\alpha$$

Simplifying,

$$Lift\ Loss = F_A(1 - \cos\alpha)$$

To determine the percent of lift loss the following equation is used.

$$\%Lift\ Loss = \frac{F_A(1 - \cos\alpha)}{F_A}$$

The location of the deformed wing is determined from the results of the static analyses of each case in FEM.

11. Results

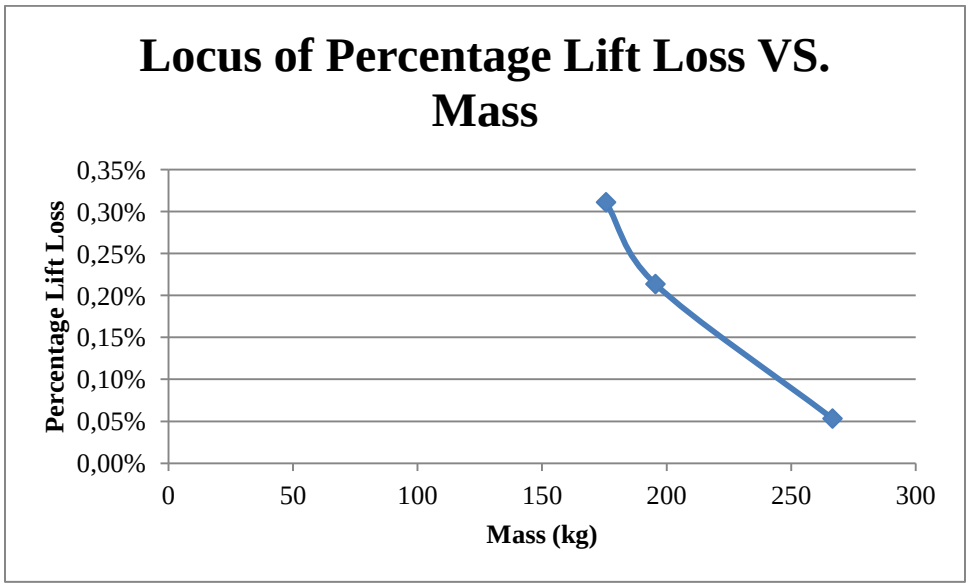

Figure 36 – Locus of percentage lift loss vs. deflection

Table 13 – Lift loss results data table

Case	Actual Deflection	Mass	Mass Loss	Lift loss percent
500 mm	500	267	+6.3%	- 0.05%
1m	1000	196	-22%	-0.21%
2m	1206	176	-30%	-0.31%

The study shows that the actual lift loss is almost negligible but has a strong mass savings at more flexible wing configurations. There is a reduction of almost 30% with a loss of only 0.31% of the lift.

12. Conclusion

This thesis has investigated a feasible structural design for the DAAP model from which to launch the optimization cases. The structure is feasible since it had only 0.94 for the failure index; this indicates that the structure has not yet failed. The model also passes buckling with a minimum value of 1.1.

For the study of operability, lift loss vs. mass data has been collated and is ready for analysis. The greatest mass savings being -30%, there was only a marginal lift loss of 0.3

13. Closing Remarks

There was an excellent reduction in mass with little affect on lift. The airfoil selection increased the mass when accounting for the curvature change in the lower wing cover. The sensitivity of the DAAP model to the mass and lift loss could improve the fidelity of the process.

14. References

[1] Engblom W.A. (2012). Novel Approach to High-Altitude Long Endurance Stationkeeping. AIAA 2012-3203.

[2] McKee E. M. (2012). *Novel Design for the Dual Aircraft Atmospheric Platform Flight Concept*. Embry-Riddle Aeronautical University, Daytona Beach, FL.

[3] Hagenauer, B. (2014). *NASA Global Hawk Ready for Atmospheric Chemistry Study :(Video: NASA Deploys ATTREX to Guam to Study Climate Change*). NASA. Retrieved from http://www.nasa.gov/centers/dryden/Features/globalhawk_attrex.html

[4] Gutro, R., & Hagenauer, B. (2014). *NASA's Global Hawks Mark 100th NASA Flight Milestone.* NASA. Retrieved from http://www.nasa.gov/centers/dryden/Features/Global_Hawk_completes_100th_flight.html

[5] NASA. (2004). *Investigation of Helios Prototype Aircraft Mishap*.

[6] "Solar Impulse HB-SIA." *SOLAR IMPULSE*. N.p., n.d. Web. 05 Feb. 2014. <http://www.solarimpulse.com/en/airplane/hb-sia/#.UvMH5bSgSE4>.

[7] Venkataraman, S., & Haftka, R.T. (2004) Structural Optimization Complexity and what has Moore's Law Done for Us?.

[8] Le Riche, R., & Haftka, R. T. (1993). Optimization of Laminate Stacking Sequence for Buckling Maximization by Genetic Algorithm. *AIAA Journal*, *Vol. 31*(No. 5), 951.

[9] Chase, N., "Optimization of Laminated Composite Aircraft Structures," Red Cedar Technology, AB-2034, East Lansing, MI.

[10] Lee, J. W., "Development of Multidisciplinary Design Optimizatino Process for a Large Scale Composite Wind Turbine Blade." Embry-Riddle Aeronautical University 2011

[11] (2014) Retreived from Nomenclaturo.com

[12] Niu, M. C. Y. (1988). *Airframe Structural Design: Practical Design Information and Data on Aircraft Structures(*2nd Ed.*)*. Hong Kong: Hong Kong Cnmilit Press LTD.

[13] Mechanical Properties of Carbon Fibre Compsoite Materials, Fibre / Epoxy resin (120°C composites.com/carbonfibre/mechanicalproperties_2.asp

[14] "HEEDS' Exclusive Search Technologies." Discover Better Designs, Faster. N.p., n.d. Web. 22 June 2012. <http://www.redcedartech.com/products/heeds_mdo/heeds_exclusive_search_technologies>.

Appendix A – Summarized Optimization Results for Each case

- Table of results for the ply thicknesses of each configuration of the design.

	Variable	Baseline (mm)	500mm	1m	2m
C1	C1_T0	1,00	3,00	1,03	0,77
	C1_T45	1,00	0,64	0,64	0,59
	C1_T90	1,00	0,41	0,41	0,39
	C1_T_Core	7,00	6,61	6,61	6,16
	Total	15,00	15,99	12,05	10,82
C2	C2_T0	1,00	1,50	0,95	0,95
	C2_T45	0,25	0,30	0,30	0,30
	C2_T_Core	5,00	3,93	3,93	3,93
	Total	8,00	8,11	7,01	7,01
C3	C3_T0	1,00	1,18	0,47	0,27
	C3_T90	0,25	0,40	0,40	0,39
	C3_T_Core	5,00	5,68	5,37	5,30
	Total	7,50	8,84	7,11	6,63
S1	S1_T0	0,25	0,48	0,48	0,48
	S1_T45	1,00	0,59	0,59	0,58
	S1_T90	0,25	0,44	0,42	0,39
	S1_T_Core	5,00	3,88	3,76	1,98
	Total	10,00	8,09	7,92	6,04
S2	S2_T0	0,25	0,47	0,49	0,47
	S2_T45	1,00	0,41	0,44	0,41
	S2_T_Core	5,00	4,51	4,51	4,51
	Total	9,50	7,08	7,24	7,08
S3	S3_T45	1,00	0,61	0,61	0,57
	S3_T_Core	5,00	4,00	2,32	0,56
	Total	9,00	6,44	4,76	2,86
R1	R1_T_45	0,25	0,31	0,31	0,31
	R1_T_Core	5,00	2,30	2,90	1,73
	Total	6,00	4,15	4,15	2,98
R2	R2_T_45	0,25	0,32	0,32	0,31
	R2_T_Core	5,00	0,88	0,88	0,88
	Total	6,00	2,17	2,13	2,13
R3	R3_T_45	0,25	0,37	0,37	0,37
	R3_T_Core	5,00	1,00	1,00	0,91
	Total	6,00	2,48	2,48	2,39

Below are images of the results from the HEEDS optimization program for each of the cases.

Tabulated Results of the 500 mm case

Study_1: Design Table

Design Id	mass	Failure_Index	EigenValue	ABS_EIG	Deflection	performance	C1_T0	C1_T45	C1_T90	C1_T_Core
245	266.613	0.28671	-1.53332	1.53332	499.795	-1.36592	3	0.64	0.41	6.605
262	266.945	0.28668	-1.53334	1.53334	499.762	-1.36763	3	0.64	0.41	6.605
250	267.688	0.28671	-1.53332	1.53332	499.59	-1.37143	3	0.64	0.41	6.605
255	269.741	0.28671	-1.5679	1.5679	495.433	-1.38195	3	0.64	0.41	6.605
254	270.643	0.28595	-1.52939	1.52939	498.843	-1.38657	3	0.64	0.5136	6.605
225	271.926	0.28741	-1.58271	1.58271	499.064	-1.39314	3	0.64	0.41	7.6766
244	266.703	0.28671	-1.53388	1.53388	500.841	-1.3947	3	0.64	0.41	6.605
188	272.418	0.28741	-1.61165	1.61165	498.996	-1.39567	3	0.64	0.41	7.6766
243	272.485	0.28741	-1.58271	1.58271	499.06	-1.39601	3	0.64	0.41	7.6766
252	272.55	0.28671	-1.76923	1.76923	495.27	-1.39634	3	0.64	0.41	6.605
226	272.569	0.28741	-1.61165	1.61165	498.996	-1.39644	3	0.64	0.41	7.6766
203	272.598	0.28741	-1.61257	1.61257	498.996	-1.39659	3	0.64	0.41	7.6766
253	272.633	0.2874	-1.58271	1.58271	499.056	-1.39677	3	0.64	0.41	7.6766
228	271.663	0.28935	-1.61217	1.61217	500.463	-1.40035	2.9803	0.64	0.41	7.9445
231	273.352	0.28731	-1.55872	1.55872	499.587	-1.40045	3	0.64	0.41	7.6766
236	273.673	0.2874	-1.52959	1.52959	498.386	-1.40209	3	0.64	0.4359	7.54265
202	274.351	0.28741	-1.63433	1.63433	496.269	-1.40556	3	0.64	0.41	7.6766
265	276.012	0.29318	-1.53773	1.53773	498.994	-1.41407	3	0.64	0.41	12.9007
229	276.028	0.28741	-2.17947	2.17947	498.79	-1.41416	3	0.64	0.41	7.6766
256	266.028	0.28671	-1.53332	1.53332	501.203	-1.42077	3	0.64	0.41	6.605
204	277.663	0.28741	-1.62934	1.62934	497.733	-1.42254	3	0.64	0.41	7.6766

This is the design table of the results for the 500mm case. The results displayed are the design ID number and the data associated. The table is arranged by the best performance of the design; this means the design with the lowest mass while meeting all of the constraints. In the case of the 500mm, the best design is design ID 245 with a mass of 266.613kg

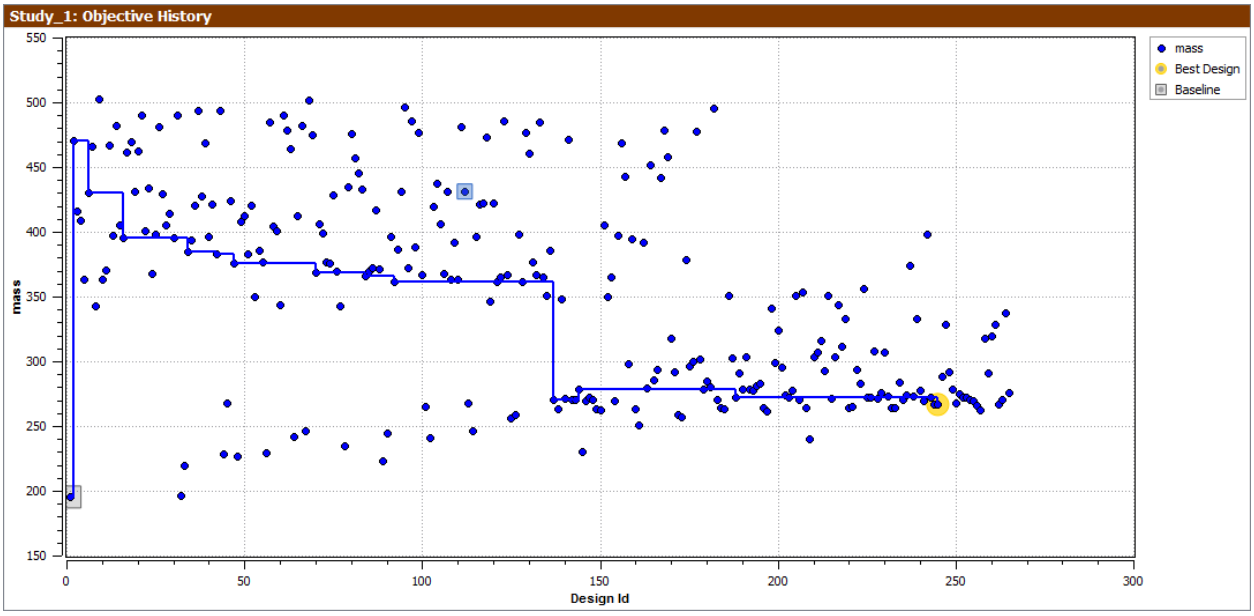

Graphic of the mass history of the 0.5m case

This is a picture of the mass history of the designs. The horizontal axis is the number of the design and the y axis is the corresponding mass. A line is traced between the best feasible designs. Best designs are characterized with minimizing mass while respecting the constraints. The mass history is for the 500mm case. The yellow circle around the design represents the design considered to be the best design by HEEDS.

Tabulated Results of the 1m case

Study_1: DesignTable_5

Design Id	mass	Failure_Index	EigenValue	ABS_EIG	Deflection	performance	C1_T0	C1_T45	C1_T90	C1_T_Core
126	194.921	0.72641	-1.10331	1.10331	1000.24	-0.77759	1.03	0.64	0.41	6.605
124	194.632	0.72814	-1.10441	1.10441	1000.54	-0.778757	1.03	0.64	0.41	6.605
113	195.51	0.72674	-1.10733	1.10733	999.563	-0.779339	1.03	0.64	0.41	6.605
122	194.62	0.72792	-1.09947	1.09947	1000.36	-0.779435	1.03	0.64	0.41	6.605
115	195.544	0.72792	-1.10445	1.10445	1000.36	-0.78079	1.03	0.64	0.41	6.605
79	195.327	0.72822	-1.10442	1.10442	1000.54	-0.781522	1.03	0.64	0.41	6.605
114	195.789	0.72807	-1.10427	1.10427	1000.52	-0.783106	1.03	0.64	0.41	6.605
123	197.992	0.72535	-1.10733	1.10733	999.204	-0.789232	1.03	0.64	0.41	6.605
91	198.267	0.72822	-1.10442	1.10442	972.757	-0.79033	1.03	0.64	0.41	6.605
98	198.269	0.72822	-1.19594	1.19594	969.642	-0.790339	1.03	0.64	0.41	6.605
107	199.654	0.72966	-1.14295	1.14295	999.182	-0.795859	1.03	0.64	0.41	6.605
77	196.475	0.72269	-1.09864	1.09864	999.389	-0.798541	1.03	0.64	0.46	6.605
64	196.481	0.72308	-1.09859	1.09859	999.59	-0.79962	1.03	0.64	0.46	6.605
125	201.994	0.71147	-1.19502	1.19502	957.21	-0.805186	1.03	0.64	0.59	6.605
88	202.44	0.76495	-1.10466	1.10466	976.692	-0.806965	0.97	0.64	0.41	6.605
53	204.803	0.71013	-1.1015	1.1015	992.762	-0.816386	1.03	0.64	0.46	6.605
65	206.746	0.709	-1.10151	1.10151	992.47	-0.824128	1.03	0.64	0.46	6.605
67	210.291	0.71013	-1.26297	1.26297	941.614	-0.838261	1.03	0.64	0.46	6.605
42	211.524	0.71013	-1.1015	1.1015	946.451	-0.843176	1.03	0.64	0.46	6.605
94	212.252	0.74482	-1.37933	1.37933	961.423	-0.846078	1	0.68	0.3	6.605
83	212.966	0.73972	-1.41272	1.41272	965.735	-0.848923	1	0.68	0.42	6.45

This design table is for the 1m case. There are two designs that are listed as being best designs; however, they have red numbers in the table. This means that the associated parameter has actually violated criteria, however, the violation is very small therefore HEEDS considered this design as feasible and made it the best design. Although HEEDS considers these slightly infeasible designs as feasible, these are not considered in this thesis. Therefore, the first or lightest design with a completely feasible design will be considered. The designs 126, and 124 are ignored since their deflections violate the 1m criterion. The design considered to be the best is design #113

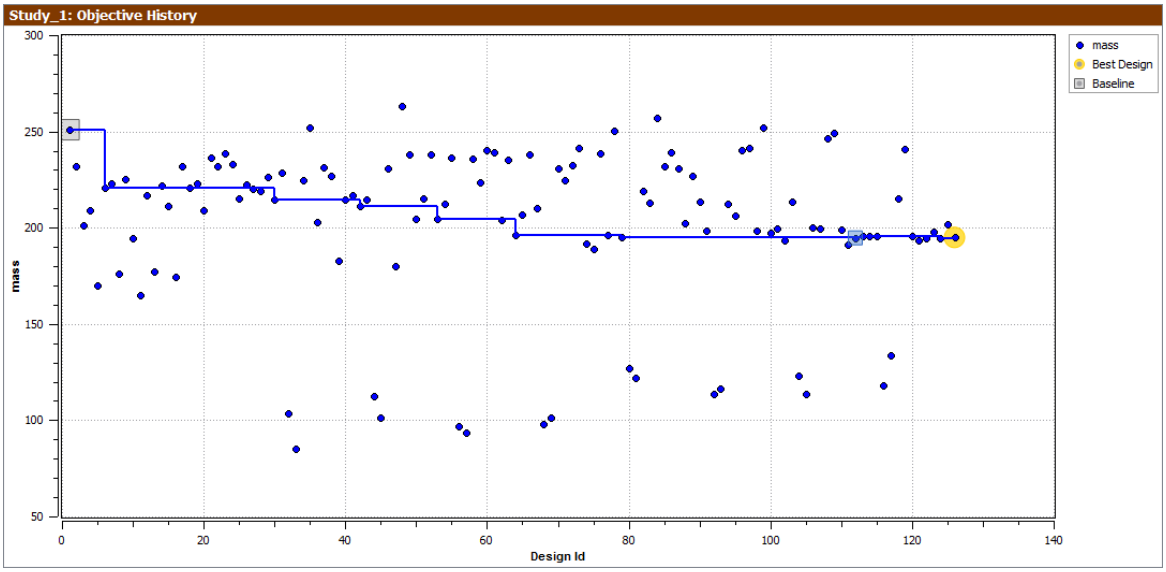

Graphic of the mass history of the 1m case

Tabulated results of the 2m case

Study_1: Design Table

Design Id	mass	Failure_Index	EigenValue	ABS_EIG	Deflection	performance	C1_T0	C1_T45	C1_T90	C1_T_Core
170	174.813	0.90923	-1.09955	1.09955	1183.49	-0.897299	0.8194	0.5854	0.3876	6.16015
153	175.049	0.90923	-1.09955	1.09955	1183.46	-0.898509	0.8194	0.5854	0.3876	6.16015
167	175.082	0.90923	-1.09955	1.09955	1183.46	-0.898677	0.8194	0.5854	0.3876	6.16015
146	175.673	0.90934	-1.09955	1.09955	1183.46	-0.901684	0.8194	0.5854	0.3876	6.16015
154	175.833	0.90934	-1.09968	1.09968	1183.43	-0.901703	0.8194	0.5854	0.3876	6.16015
133	175.706	0.90934	-1.09955	1.09955	1183.46	-0.901851	0.8194	0.5854	0.3876	6.16015
156	176.028	0.90961	-1.09974	1.09974	1182.96	-0.902401	0.8194	0.5854	0.3924	6.54145
169	174.617	0.91113	-1.09901	1.09901	1184.53	-0.90272	0.8194	0.5854	0.3876	6.16015
149	175.494	0.90934	-1.09874	1.09874	1183.46	-0.912136	0.8194	0.5854	0.3876	6.16015
155	178.475	0.94122	-1.10241	1.10241	1205.93	-0.914368	0.7726	0.5854	0.3876	6.16015
138	179.024	0.89928	-1.10182	1.10182	1178.15	-0.917186	0.8194	0.5854	0.3876	6.16015
145	179.355	0.89769	-1.10213	1.10213	1177.34	-0.91888	0.8194	0.5854	0.3876	6.16015
157	179.532	0.89757	-1.10214	1.10214	1177.29	-0.919788	0.8194	0.5854	0.3876	6.16015
139	179.598	0.89757	-1.10214	1.10214	1177.29	-0.920124	0.8194	0.5854	0.3876	6.16015
126	179.617	0.89757	-1.10214	1.10214	1177.29	-0.920221	0.8194	0.5854	0.3876	6.16015
123	180.612	0.89777	-1.10213	1.10213	1140.11	-0.925319	0.8194	0.5854	0.3876	6.16015
111	181.003	0.89757	-1.10214	1.10214	1140.03	-0.927323	0.8194	0.5854	0.3876	6.16015
110	181.161	0.89759	-1.10213	1.10213	1140.02	-0.92813	0.8194	0.5854	0.3876	6.16015
112	181.479	0.89757	-1.10214	1.10214	1132.79	-0.929762	0.8194	0.5854	0.3876	6.16015
91	181.703	0.89757	-1.10214	1.10214	1140.01	-0.930908	0.8194	0.5854	0.3876	6.16015
78	182.353	0.89755	-1.10214	1.10214	1140.01	-0.934241	0.8194	0.5854	0.3876	6.16015

This is the design table for the 2m case. Much like the 1m case there are plenty of designs considered to be best designs by HEEDS even though they violate the criteria. In this case, the deflection is not the limiting parameter, it is the buckling. The designs that violate the criteria and which will not be considered as best designs are, 170, 153, 167, 146, 154, 133, 156, 169, and 149. The lightest and first to meet all the criteria is the design 155.

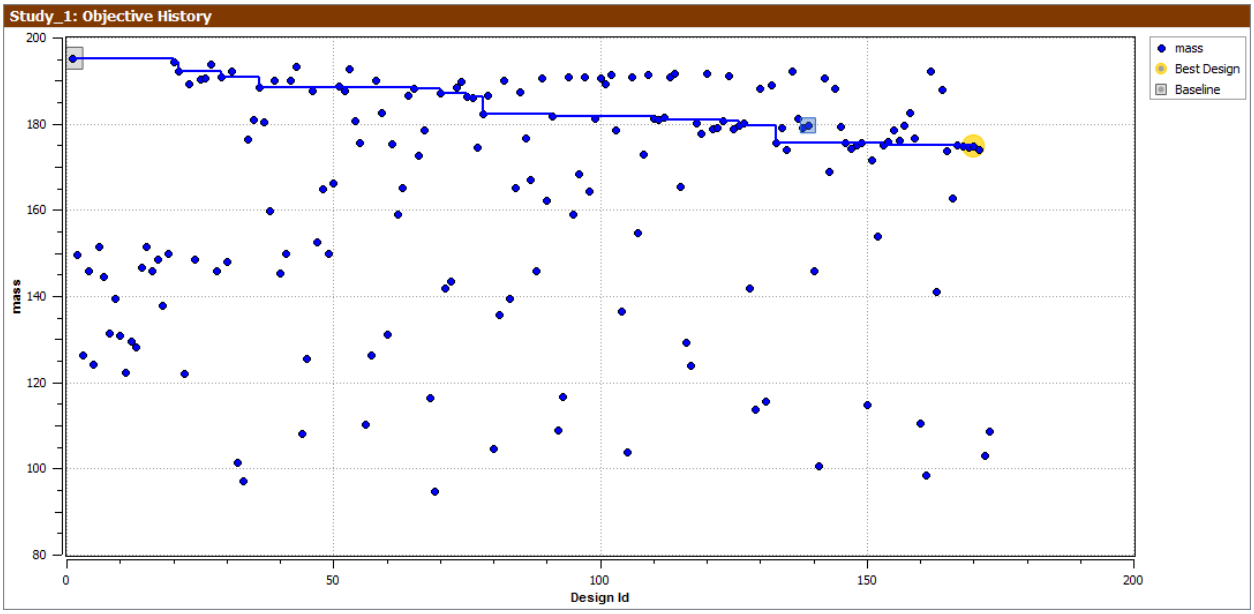

Graphic of the mass history of the 0.5m case

Appendix B – CFD to FEA MATLAB Converter

```
%t1=tic; %start timer
%CFD input in METERS
%FEA input in mm
%FEA output in mm
%FEA PTS in mm
%CFD pressure inputs in Pa
%FEA pressure output in N/mm^2 (MPa)


%flow direction positive Y
%rotation is about negative Y


% Description: This programs uses CFD mesh and nodal pressure values and
% applies them to the nearest FEA mesh node.

tic; %start timer

%********Input File Names*************
FEA1='FEA_elements.dat'; %Fea Elements file
FEA2='FEA_nodes.dat'; %Fea Nodes File
CFD='CFD_loads.dat'; %CFD Pressure Results file
FEA_LOADS='96RPM3mps_Pressure_Load_Output.dat'; %FEA PLOAD4 Output file
LOAD_VERIF='96RPM3mps_Pressure_Verification_2.dat'; %Output file to verify
loads


%------------Import FEA Data-----------------------------------------------
import_elms(FEA1);
num_elm=size(data,1); %number of elements
flag=0;
start=1;


%th=2.688/180*pi;
%R=[cos(th) 0 sin(th);0 1 0; -sin(th) 0 cos(th)];

% This sets the number of times the code runs
%num_elm=100;% For trouble shooting set to a low number ie. 1

lc=1; % load case label
tic
for i=1:num_elm %transfer element valeus to element structure

    elms(i).type=rowheaders(i);
    elms(i).id=data(i,1);

    elms(i).p1=data(i,3);
    elms(i).p2=data(i,4);
    elms(i).p3=data(i,5);
    elms(i).p4=data(i,6); %taken out for tri elements
```

```
end
import_nodes(FEA2);
num_node=size(data,1); %save number of nodes

for i=1:num_node %transfer node values to node structure

    nds(i).type=rowheaders(i);
    nds(i).id=data(i,1);
    nds(i).x=data(i,3);
    nds(i).y=data(i,4);
    nds(i).z=data(i,5);
    nds(i).flag=0; %node flag

end

NData = [data(:,1),data(:,3),data(:,4),data(:,5)];

nds_storage=nds; %store values that will be modified
num_node_storage=num_node;

x=zeros(4,1);
y=zeros(4,1);
z=zeros(4,1);

%**********************************
t1=tic;
for i=1:num_elm %loop thru elements
    flag=0;
    if strcmp(elms(i).type, 'CQUAD4')==1
                % This searches for the nodes for the elements using
                % indexing instead of loops "Phil"
                elms(i).xyz1(1)=NData(find(NData(:,1)==elms(i).p1),2);
                elms(i).xyz1(2)=NData(find(NData(:,1)==elms(i).p1),3);
                elms(i).xyz1(3)=NData(find(NData(:,1)==elms(i).p1),4);

                elms(i).xyz2(1)=NData(find(NData(:,1)==elms(i).p2),2);
                elms(i).xyz2(2)=NData(find(NData(:,1)==elms(i).p2),3);
                elms(i).xyz2(3)=NData(find(NData(:,1)==elms(i).p2),4);

                elms(i).xyz3(1)=NData(find(NData(:,1)==elms(i).p3),2);
                %fprintf('dude')
                elms(i).xyz3(2)=NData(find(NData(:,1)==elms(i).p3),3);
                elms(i).xyz3(3)=NData(find(NData(:,1)==elms(i).p3),4);

                %fprintf('dude')
                elms(i).xyz4(1)=NData(find(NData(:,1)==elms(i).p4),2);
                elms(i).xyz4(2)=NData(find(NData(:,1)==elms(i).p4),3);
                elms(i).xyz4(3)=NData(find(NData(:,1)==elms(i).p4),4);

      else
    % This searches for the nodes for the elements using
                % indexing instead of loops "Phil"
                elms(i).xyz1(1)=NData(find(NData(:,1)==elms(i).p1),2);
                elms(i).xyz1(2)=NData(find(NData(:,1)==elms(i).p1),3);
                elms(i).xyz1(3)=NData(find(NData(:,1)==elms(i).p1),4);
```

```
                elms(i).xyz2(1)=NData(find(NData(:,1)==elms(i).p2),2);
                elms(i).xyz2(2)=NData(find(NData(:,1)==elms(i).p2),3);
                elms(i).xyz2(3)=NData(find(NData(:,1)==elms(i).p2),4);

                elms(i).xyz3(1)=NData(find(NData(:,1)==elms(i).p3),2);
                %fprintf('dude')
                elms(i).xyz3(2)=NData(find(NData(:,1)==elms(i).p3),3);
                elms(i).xyz3(3)=NData(find(NData(:,1)==elms(i).p3),4);
     end


    %calculating average location and convert to meters
    if strcmp(elms(i).type, 'CQUAD4')==1

elms(i).ax=mean([elms(i).xyz1(1),elms(i).xyz2(1),elms(i).xyz3(1),elms(i).xyz4
(1)])/1000.;

elms(i).ay=mean([elms(i).xyz1(2),elms(i).xyz2(2),elms(i).xyz3(2),elms(i).xyz4
(2)])/1000.;

elms(i).az=mean([elms(i).xyz1(3),elms(i).xyz2(3),elms(i).xyz3(3),elms(i).xyz4
(3)])/1000.;
    else %tri element average

elms(i).ax=mean([elms(i).xyz1(1),elms(i).xyz2(1),elms(i).xyz3(1)])/1000.;

elms(i).ay=mean([elms(i).xyz1(2),elms(i).xyz2(2),elms(i).xyz3(2)])/1000.;

elms(i).az=mean([elms(i).xyz1(3),elms(i).xyz2(3),elms(i).xyz3(3)])/1000.;
    end



     elms(i).dx=elms(i).ax;
     elms(i).dy=elms(i).ay;
     elms(i).dz=elms(i).az;


     %elms(i).cy=elms(i).cy;
     %elms(i).cz=-elms(i).ax+.05;
     %elms(i).cz=elms(i).ax-(.08245+0.08576);


    if mod(i,1000)==0 %display progress
        clc
        disp('FEA Centroid % Progress')
        disp(i/(num_elm)*100)
    end
        clc
        disp('FEA Centroid % Progress')
        disp(i/(num_elm)*100)

    end %end of loop for elements
```

```
%------------Import CFD Data-----------------------------------------------

importfile(CFD)
X=data(:,1); %*1000;
Y=data(:,2); %*1000;
Z=data(:,3); %*1000;

% I only changed this because my axes were different from the CFD "Phil"
% X=-data(:,1);%*1000;
% Z=data(:,2);%*1000;
% Y=data(:,3);%*1000;
Press=data(:,4);

% I created a matrix with all of the data so that I could use indexing
% "Phil"
CFDID(:,1) = 1:size(X,1);
CFDdata = [CFDID X Y Z Press];

%-------------------------------------------------------------------------
%---------------FEA Node location-----------------------------------------
% fea='Turbine_Test_GridPts.txt'
% importfile(fea)
% x=data(:,3);
% y=data(:,4);
% z=data(:,5);
% node=data(:,1);

% This sets limits the number of CFD data points used for the minimum
distance
% search "Phil"

%%
RF = 10;
RG = 10;
RH = 10;
devx = (abs(max(X))+abs(min(X)))/RF;
devy = (abs(max(Y))+abs(min(Y)))/RG;
devz = (abs(max(Z))+abs(min(Z)))/RH;

%-------------------------------------------------------------------------
for k=1:num_elm

    % Reduce Sampling Size by X "I don't know why I named this Sam but this
    % is the actual process of cutting down the size of the search and
    % should be the last thing I changed "Phil"
    SamX = CFDdata(CFDdata(:,2)<= elms(k).dx + devx,:);
    SamX = SamX(SamX(:,2)>=elms(k).dx - devx,:);
%SamZ = SamX(SamX(:,2)>=elms(k).dx - devx,:);

    SamY = SamX(SamX(:,3)<=elms(k).dy + devy,:);
    SamY = SamY(SamY(:,3)>=elms(k).dy - devy,:);
```

```
    SamZ = SamY(SamY(:,4)<=elms(k).dz + devz,:);
    SamZ = SamZ(SamZ(:,4)>=elms(k).dz - devz,:);
    d = 0;
    for i=1:size(SamZ,1)   %search for the minimum distance

        d(i,1)=sqrt((SamZ(i,2)-elms(k).dx)^2 + (SamZ(i,3)-elms(k).dy)^2 +
(SamZ(i,4)-elms(k).dz)^2); %minimum distances

    end

[elms(k).min,elms(k).I]=min(d);%returns the minimum value and its location
% Pressure=Press(I);%the pressure that corisponds to the minimum distance
% output(k,1)=node(k);
% output(k,2)=x(k);
% output(k,3)=y(k);
% output(k,4)=z(k);
%output(k,5)=Pressure;

elms(k).press=SamZ((elms(k).I),5);
% SamX = 0;
% SamY = 0;
% SamZ = 0;


        clc
            disp('Pressure Search % Progress')
            disp(k/(num_elm)*100)
end

%write out pressure load cards
fid = fopen(FEA_LOADS, 'w');
for i=1:num_elm
    fprintf(fid, 'PLOAD4
%8i%8i%8.5f\n',lc,elms(i).id,elms(i).press/1000000); % convert the pressure
to MPA (N/mm^2) and invert direction
end
fclose(fid);

%write out pressure verification file
fid = fopen(LOAD_VERIF, 'w');
fprintf(fid, '***Pressures in Pascals, Locations in meters\n');
 fprintf(fid, '     X       Y       Z       P\n');
for i=1:num_elm
    fprintf(fid, '%8.4f%8.4f%8.4f%8.0f\n',
elms(i).dx,elms(i).dy,elms(i).dz,elms(i).press); % pressures for mikes
verification
end
fclose(fid);

disp('done');
toc(t1)
%plot data
plot3(CFDdata(:,2),CFDdata(:,3),CFDdata(:,4));
axis([-5 5 0 15 -7 7]);
```

Appendix C – Failure index code (For reading .f06 files generated by NASTRAN)

```
tic
clc
clear all
close all


tic; %start timer

%********Input File Names*************
FEA1='FEA_elements.dat'; %Fea Elements file
FEA2='FEA_nodes.dat'; %Fea Nodes File
CFD='CFD_loads.dat'; %CFD Pressure Results file
FEA_LOADS='96RPM3mps_Pressure_Load_Output.dat'; %FEA PLOAD4 Output file
LOAD_VERIF='96RPM3mps_Pressure_Verification_2.dat'; %Output file to verify
loads
FEA3='Complete_Wing_Box_Model.f06'; %FEA stress file
OUT1='FEA_stresses_Extracted.dat';


%------------Import FEA Data-----------------------------------------------

% Automatic Pick File
fid = fopen('model000.f06','r');

A = textscan(fid,'%s','delimiter','\n');
fclose(fid);
n = length(A{:});
D = [0];
Begin_data = 9882;
End_data = 82981;
% Truncate data at the Strain elements
Start = ('S T R A I N S   I N   L A Y E R E D   C O M P O S I T E   E L E M E
N T S   ( Q U A D 4 )');

counter = 0;
% Filter Data
for i = Begin_data:End_data
    B = A{:}{i,:};
    [C, OK] = str2num(B);
        if OK == 1 && C(1) >0
            Clength = size(C,1);
            Cwidth = size(C,2);
            Dlength = size(D,1);
            Dwidth = size(D,2);
            % create the Contatenaed matrix
            E = zeros(Dlength+Clength,Cwidth);
            E(1:Dlength,1:Dwidth) = D;
            E(Dlength+1:Dlength+Clength,1:Cwidth) = C;
            %Reset Values Matrix
            D = E;
            counter = counter + 1;
            clc
            disp(counter)
```

```
        end
end


R(:,:) = D(9:length(D)-1,:);

%%
% Mechanical Properties
F1t = 750; %MPa
F1c = 600; %MPa
F2t = 25; %MPa
F2c = 125; %MPa
F6  = 35; %MPa
% Tsai-Wu Factors
f1  = 1/F1t - 1/F1c;
f11 = 1/F1t/F1c;
f2  = 1/F2t - 1/F2c;
f22 = 1/F2t/F2c;
f12 = -0.5*sqrt(f11*f22);
f66 = 1/F6/F6;

% Criteria
for i = 1:57104 %1:length(R); This is what it should be but I dont have the
time for now it is just the last element of the stress section
Sig1 = R(i,3); %Stress fiber direction
Sig2 = R(i,4); %Stress matrix direction
tau6 = R(i,5); %Shear stress

Criteria(i,1) = f1.*Sig1 + f2.*Sig2 + f11.*Sig1^2 + f22.*Sig2^2 +f66.*tau6^2
+ 2.*f12.*Sig1.*Sig2;
end

Max_Failure_Index = max(Criteria)
RI_Critical_Element = find(Criteria == Max_Failure_Index);
Element = R(RI_Critical_Element,1)
Ply = R(RI_Critical_Element,2)

fid = fopen('Failure_Index.dat','wt');
fprintf(fid,'%8.4e\n',Max_Failure_Index);
fclose(fid);

toc
quit
```